

# **ESTIMATION OF AERODYNAMICS EFFECT ON LOW RISE DOMICAL STRUCTURES**

A DISSERTATION  
SUBMITTED IN PARTIAL FULFILLMENT OF THE  
REQUIREMENTS FOR THE AWARD OF THE DEGREE  
of  
MASTER OF TECHNOLOGY  
in  
STRUCTURAL ENGINEERING

Submitted by :

**JYOTI SINGH**

**(2K20/STE/10)**

Under the supervision of

**Dr. RITU RAJ**

(Assistant Professor, Department of CE, DTU)



**DEPARTMENT OF CIVIL ENGINEERING**

**DELHI TECHNOLOGICAL UNIVERSITY**

(Formerly Delhi College of Engineering)

Bawana Road, Delhi – 110042

MAY 2022

# **ESTIMATION OF AERODYNAMICS EFFECT ON LOW RISE DOMICAL STRUCTURES**

A DISSERTATION  
SUBMITTED IN PARTIAL FULFILLMENT OF THE  
REQUIREMENTS FOR THE AWARD OF THE DEGREE  
of  
MASTER OF TECHNOLOGY  
in  
STRUCTURAL ENGINEERING

Submitted by :

**JYOTI SINGH**

**(2K20/STE/10)**

Under the supervision of

**Dr. RITU RAJ**

(Assistant Professor, Department of CE, DTU)



**DEPARTMENT OF CIVIL ENGINEERING**

**DELHI TECHNOLOGICAL UNIVERSITY**

(Formerly Delhi College of Engineering)

Bawana Road, Delhi – 110042

MAY 2022

## **DELHI TECHNOLOGICAL UNIVERSITY**

(Formerly Delhi College of Engineering)  
Bawana Road, Delhi-110042

### **CANDIDATE'S DECLARATION**

I Jyoti Singh, Roll No. 2K20/STE/10 of M.Tech (Structural Engineering), hereby declare that the project Dissertation titled “Estimation of aerodynamics effect on low rise domical structures” which is submitted by me to the Department of Civil Engineering, Delhi Technological University, Delhi in partial fulfilment of the requirement for the award for the degree of Master of technology, is original and not copied from any source without proper citation. This work has not previously formed the basis for the award of any Degree, Diploma Associateship , Fellowship or other similar title or recognition.



Place: Delhi

JYOTI SINGH

Date:30/05/2022

**DEPARTMENT OF CIVIL ENGINEERING**

**DELHI TECHNOLOGICAL UNIVERSITY**

(Formerly Delhi College of Engineering)

Road, Delhi-110042

**CERTIFICATE**

I hereby certify that the Project Dissertation titled “Estimation of aerodynamics effect on low rise domical structures” which is submitted by Jyoti Singh, 2K20/STE/10 Department of Civil Engineering (Structural Engineering), Delhi Technological University Delhi in partial fulfilment of the requirement for the award of the degree of the Master of Technology, is a record of the project work carried out by the student under my supervision. To the best of my knowledge this work has not been submitted in part or full for any Degree or Diploma to this University or elsewhere.



Place : Delhi

Dr. RITU RAJ

Date:30/5/2022

**SUPERVISOR**

## **ACKNOWLEDGEMENT**

I would like to express my sincere gratitude to my supervisor **Dr. Ritu Raj** (Department of Civil Engineering, Delhi Technological University) for the continuous support of my M.Tech study and research, for his patience, motivation, enthusiasm, immense knowledge. The guidance he provided helped me throughout the research and writing process of my thesis.

I owe a deep sense of gratitude to PhD Scholar **Rahul Kumar Meena** for his keen interest at every stage of this research. It was his prompt inspiration and timely suggestions that enabled me to finish my thesis.

I would express my deepest and sincere appreciation to my family for their continual emotional and financial support. They have always remained my source of encouragement. I am also very thankful to my friends who always encouraged me and supported me. I could not have completed this thesis without the support, push, and good wishes of everyone mentioned above.

**JYOTI SINGH**

## ABSTRACT

The wind is a complex phenomenon because of the many flow situations that result from wind interaction with structures. In designing buildings, it is important to take wind into account, since this is one of the more significant forces of nature. In time and space, the characteristics of wind-induced loads on buildings continually change. A building's design depends on predicting the actual effects of turbulent wind forces to account for the most critical design scenarios that may occur during a specific design period. Low-rise structures are susceptible to high winds alike tall structures. These low-rise structures are exposed to the atmospheric wind speed that is highly prone to uplift pressure. The present study demonstrates the investigation of mean wind pressure on isolated domical low-rise buildings, and the arrangement of domical low-rise buildings in a T-shape and L shape. The wind incidence angle is varied from  $0^\circ$  to  $180^\circ$  at an interval of  $30^\circ$  for T shape and  $0^\circ$  to  $360^\circ$  at an interval of  $30^\circ$  because of the asymmetric plan and the spacing between the buildings is varied at a distance of  $0$ ,  $b/2$ ,  $b$ ,  $3b/2$  and  $2b$  where  $b$  is the width of the isolated building i.e.  $0\text{mm}$ ,  $50\text{mm}$ ,  $100\text{mm}$ ,  $150\text{mm}$  and  $200\text{mm}$ . We performed the numerical analysis using ANSYS CFX using the shear stress transport turbulence model. The pressure distribution over the surfaces using Coefficient of pressure ( $C_p$ ) and velocity streamlines are analyzed for each building model, and the effect of interference on surrounding buildings is studied. The finding is useful for structural engineers when designing the structure of a low-rise building and the outcome of the study is depicted by pictorial and tabular representation. Interestingly, the maximum positive wind pressure coefficients were

found on the windward side of the dome, whereas the maximum negative wind pressure coefficients occurred at the apex. The interference research was carried out in order to comprehend the consequences of various conditions that may emerge in real-life scenarios, and it was found that the maximum negative pressure is found to be on the centre of the domes which are directly hit by the wind and the value is found to be decrease in the corner region. For the variation of spacing, the average coefficient of pressure acting on each dome was found, and it was observed that the average pressure acting on the dome surface is suction for isolated, L shape and T shape domical roofs. The finding is useful for structural engineers when designing the structure of a low-rise building. As a result, it is important for designers and planners to study the wind induced response of the buildings.

## TABLE OF CONTENTS

<b>CANDIDATE’S DECLARATION .....</b>	<b>ii</b>
<b>CERTIFICATE .....</b>	<b>iii</b>
<b>ACKNOWLEDGEMENT .....</b>	<b>iv</b>
<b>ABSTRACT .....</b>	<b>v</b>
<b>LIST OF TABLES .....</b>	<b>x</b>
<b>LIST OF FIGURES .....</b>	<b>xi</b>
<b>CHAPTER 1 INTRODUCTION .....</b>	<b>1</b>
1.1 GENERAL .....	1
1.2 ROOFS .....	3
1.3 EVALUATION PROCEDURES .....	4
1.3.1 Wind tunnel testing .....	4
1.3.2 CFD .....	4
1.3.3 Codal provisions .....	4
1.4 NEED OF PROPOSED STUDY .....	4
1.5 OBJECTIVE OF THE STUDY .....	5
1.6 LIMITATIONS OF THE STUDY .....	5
<b>CHAPTER 2 LITERATURE REVIEW .....</b>	<b>6</b>
2.1 INTRODUCTION .....	6
2.2 LITERATURE REVIEW .....	6
2.3 LITERATURE GAP .....	10
<b>CHAPTER 3 VALIDATION .....</b>	<b>11</b>



3.1 GENERAL .....	11
3.2 DETAILS OF MODEL .....	11
3.3 NUMERICAL ANALYSIS .....	13
3.4 RESULTS .....	15
<b>CHAPTER 4 WIND RESPONSE ANALYSIS .....</b>	<b>16</b>
4.1 GENERAL .....	16
4.2 DETAILS OF MODEL .....	16
4.3 DETAILS OF WIND TUNNEL .....	22
4.3.1 COMPUTATIONAL DOMAIN .....	22
4.4 SHEAR STRESS TRANSPORT MODEL .....	25
<b>CHAPTER 5 RESULTS .....</b>	<b>26</b>
5.1 GENERAL .....	26
5.2 ISOLATED BUILDING .....	26
5.2.1 COEFFICIENT OF PRESSURE ( $C_p$ ) .....	26
5.2.2 VELOCITY STREAMLINES .....	28
5.3 BUILDING ARRANGED IN T- SHAPE CONFIGURATION .....	30
5.3.1 COEFFICIENT OF PRESSURE ( $C_p$ ) .....	30
5.3.2 VELOCITY STREAMLINES .....	35
5.4 BUILDING ARRANGED IN L- SHAPE CONFIGURATION .....	41
5.4.1 COEFFICIENT OF PRESSURE ( $C_p$ ) .....	41
5.4.2 VELOCITY STREAMLINES .....	46
<b>CHAPTER 6 CONCLUSION .....</b>	<b>54</b>
<b>REFERENCES .....</b>	<b>56</b>

**PUBLICATIONS .....60**

## **LIST OF TABLES**

Table 3.1 Comparative study of results from ANSYS CFX and IS code 875 Part 3	15
Table 5. 1 Coefficient of pressure ( $C_p$ ) for T shape configuration at 0 mm spacing	30
Table 5. 2 Coefficient of pressure ( $C_p$ ) for T shape configuration at 50 mm spacing	31
Table 5. 3 Coefficient of pressure ( $C_p$ ) for T shape configuration at 100 mm spacing	32
Table 5. 4 Coefficient of pressure ( $C_p$ ) for T shape configuration at 150 mm spacing	33
Table 5. 5 Coefficient of pressure ( $C_p$ ) for T shape configuration at 200 mm spacing	34
Table 5. 6 Coefficient of pressure ( $C_p$ ) for L - shape configuration at 0 mm spacing	41
Table 5. 7 Coefficient of pressure ( $C_p$ ) for L shape configuration at 50 mm spacing	42
Table 5. 8 Coefficient of pressure ( $C_p$ ) for L shape configuration at 100 mm spacing	43
Table 5. 9 Coefficient of pressure ( $C_p$ ) for L shape configuration at 150 mm spacing	44
Table 5. 10 Coefficient of pressure ( $C_p$ ) for L shape configuration at 200 mm spacing	45

## LIST OF FIGURES

Fig 3.1 Dimensions of the Validation model in mm	12
Fig 3. 2 Computational domain used for CFD simulation	12
Fig 3.3 Cp contours for the validation model	14
Fig 3.4 Cp values of curved roof as per IS 875 Part 3 (2015) clause 7.3.3.6	14
Fig 4. 1 Dimensions of the isolated building model in mm	17
Fig 4. 2 Plan and Isometric view of arrangement of domical roof buildings in T shape at 0 mm spacing	17
Fig 4. 3 Plan and Isometric view of arrangement of domical roof buildings in T shape at 50 mm spacing	18
Fig 4. 4 Plan and Isometric view of arrangement of domical roof buildings in T shape at 100 mm spacing	18
Fig 4. 5 Plan and Isometric view of arrangement of domical roof buildings in T shape at 150 mm spacing	19
Fig 4. 6 Plan and Isometric view of arrangement of domical roof buildings in T shape at 200 mm spacing	19
Fig 4. 7 Plan and Isometric view of arrangement of domical roof buildings in L shape at 0 mm spacing	20
Fig 4. 8 Plan and Isometric view of arrangement of domical roof buildings in L shape at 50 mm spacing	20
Fig 4. 9 Plan and Isometric view of arrangement of domical roof buildings in L shape at 100 mm spacing	21
Fig 4. 10 Plan and Isometric view of arrangement of domical roof buildings in L shape at 150 mm spacing	21
Fig 4. 11 Plan and Isometric view of arrangement of domical roof buildings in L shape at 200 mm spacing	22

Fig 4. 12 Model and the computational domain used for simulation in ANSYS (dimensions in mm)	24
Fig 4.13 Tetrahedral meshing used for CFD simulation	24
Fig 5. 1 Pressure contours on the isolated building	27
Fig 5. 2 Cp contours for the isolated building model	27
Fig 5. 3 Velocity Streamlines for isolated building model	29
Fig 5. 4 Streamlines for T shape arrangement at 0 mm spacings	36
Fig 5. 5 Streamlines for T shape arrangement at 50 mm spacing	37
Fig 5. 6 Streamlines for T shape arrangement at 100 mm spacings	38
Fig 5. 7 Streamlines for T shape arrangement at 150 mm spacings	39
Fig 5. 8 Streamlines for T shape arrangement at 200 mm spacings	40
Fig 5. 9 Streamlines for L shape arrangement at 0mm spacing	48
Fig 5. 10 Streamlines for L shape arrangement at 50mm spacing	49
Fig 5. 11 Streamlines for L shape arrangement at 100mm spacing	50
Fig 5. 12 Streamlines for L shape arrangement at 150 mm spacing	51
Fig 5. 13 Streamlines for L shape arrangement at 200 mm spacing	52
Fig 5. 14 Average Cp variation for different spacing between the buildings	53

# **CHAPTER 1**

## **INTRODUCTION**

### **1.1 GENERAL**

There are many new structures being constructed right now that are wind-sensitive because they are thin, slender, flexible, large, lightweight and often curved. In addition to these factors, a variety of materials are also used which are stressed to a higher percentage of their ultimate strength than in former days because of better assurance of materials.

The movement of air along a particular direction in the atmosphere is called wind. The behaviour of structure should be depending upon the characteristics of the wind. The wind can be divided into two categories, rotating and non-rotating wind. Tornadoes and tropical cyclones produce rotating winds. Winds with non-rotating directions arise from differences in pressures. This is called the pressure system of the wind. The wind can be persist for the distance 50 — 100 kms known as fully developed pressure system winds. Under storms winds always move highly speed for a few minutes. Because the sun's radiations are reflected at different latitudes, and land areas heat and cool more rapidly than the sea, winds are caused by air temperature differences on the earth's surface. The temperatures up-downs always due to pressure of air.

The motion of wind is opposed near the earth surface. The speed of wind is reduced due to the surface friction. The speed of wind starts from zero and increases with increases in elevation and at some height known as the gradient height where friction due to earth surface has no influence on it, and will attains its “gradient velocity”.

The pressure of the air strike the surface of the structure, it will exert force on it. We refer to these forces as wind loads. There may be components of force in the directions other than the direction of wind. Drag force along a direction is the component of force; lift force (crosswind force) and side force (transverse force) along a normal direction are components of force. A moment that bends the structure in the direction of the wind is called an overturning moment, a moment that twists the structure about a vertical axis is called torque and a moment which bends it in the transverse direction is called a sideways moment. Globally, low-rise buildings for industrial, residential, and other purposes, as well as high-rise buildings, may be considered to make up a majority of structures. Low-rise structures are more at risk from heavy winds alike tall structures that have been built. Flat roofs are the most common type of low-rise roof, followed by mono-slope roofs arched roofs, gable roofs, hip roofs, multi-span gable roofs, pyramidal roofs, saw-tooth roofs, mansard roofs, troughed roofs, curved roofs, stepped roofs and canopy roofs.

These roofed buildings are subjected to considerable wind loads on the roof structures due to their exposure to atmospheric wind speed. High wind-induced suctions can cause extensive damage, including rain intrusion and the loss of internal building materials. As a result, in addition to other loads, the wind load should be incorporated into the structure's design.

Wind causes random time-dependent loads, which can be thought of as mean plus fluctuating waves. Due to the fluctuating component (gustiness) of the wind, all structures will experience dynamic oscillations. For rigid structures, the oscillations are insignificant, and as such the static pressure can be viewed satisfactorily as equivalent. If a structure's natural time period is less than one second, it is considered short and rigid. The more flexible systems, such as tall buildings, react dynamically to wind gusts.

To determine the flow pattern and complete the design in accordance with it, a wind tunnel model study is required.

## **1.2 ROOFS**

As the top covering of a building, a roof comprises the materials and structures necessary to support it on the walls and uprights, insuring protection from wind, sunlight, rain, and temperature extremes. Roofs are part of the envelope of a building.

Roofing materials, local construction traditions, and more general concepts of architectural design and practice determine the quality of a roof, as does local or national legislation, as well as the purpose of the building that it covers. A roof is primarily used to protect a building from rain in most nations.

The roof assembly serves multiple purposes. Some of them include:

1. A roof's purpose is to shed water, or to avoid pools of water on the surface. Standing water on the roof surface will increase the live load on the roof structure, which is dangerous. In addition, standing water speeds up the degradation of most roofing materials.
2. Roofs should be smooth and free of blemishes. Some roofs are not just chosen for their function, but also for their beauty, much like the cladding on walls.
3. In order to prevent the interior of the structure from being affected by weather factors such as rain, wind, sun, heat, and snow.
4. In order to act as thermal insulation.
5. Designed to last the expected service life.

Various environmental factors have an impact on the shape of roofs, along with the materials available for roof structure and covering.

There are several types of roof shapes, including flat, mono-pitch, gabled, mansard, hipped, butterfly, arched, and dome. They differ in numerous ways.



### **1.3 EVALUATION PROCEDURES**

**1.3.1 Wind tunnel testing** is one method for investigating wind loads on buildings. However, this is a time-consuming and costly procedure that necessitates a significant amount of work and has a variety of limitations, including varied scale ratios and complicated turbulent structures, wind pulsation, and difficulty in simulating high Reynolds numbers.

**1.3.2 CFD** saves a lot of time in design and research by giving precise and aesthetically pleasing data. CFD simulations have been adopted instead of wind tunnel testing in a number of studies, and the results for wind loads produced from CFD simulations are nearly identical to experimental results. The modelling flexibility is one of the key benefits of computer-based methods over wind tunnels and field research. The inflow parameters and model shape may be easily modified on the computer, allowing for the exploration of a wide range of effects that would otherwise be costly and time-consuming using traditional methods.

**1.3.3 Codal provisions** IS 875 part 3 ,geometry of roofs is one of the limitations. It is commonly accepted that the codal provision of IS 875 (part 3) limits the coefficient of pressure  $C_p$  values to 0 and 90 degree wind incidence angles, and to standard-shaped buildings only. So, wind tunnel experiments are conducted to measure wind loads so as to obtain more reliable results than codes.

### **1.4 NEED OF PROPOSED STUDY**

Low-rise structures are more susceptible to high winds alike tall structures. These low-rise structures are exposed to the atmospheric wind speed that is highly prone to uplift pressure. The finding is useful for structural engineers when designing the structure of a low-rise building.

The standard codes for wind induced response offer only limited assistance to the designer for calculation of the interference effect. The research was carried out on the effects of wind loads on low-rise buildings in the presence of a building nearby. It is commonly accepted that the codal provision of IS 875 (part 3) limits the coefficient of

pressure  $C_p$  values to  $0^\circ$  and  $90^\circ$  wind incidence angles, and to standard-shaped buildings only. So, wind tunnel experiments are conducted to measure wind loads so as to obtain more reliable results than codes.

Buildings located in realistic environments may experience wind loads that differ significantly from buildings situated in isolated environments, according to several researchers. The flow-induced forces on a building can be decreased or increased based on the distance from the neighbouring structures, the direction of the flow direction, and region conditions upstream and the geometry and plan of the building or structures. As a result, designers and planners must consider this effect, commonly known as interference.

### **1.5 OBJECTIVE OF THE STUDY**

- To evaluate the effect of peak wind pressure on the low rise building.
- To investigate the effect of interference on a building when multiple buildings are placed in an L-shape configuration at different spacing.
- To investigate the effect of interference on a building when multiple buildings are placed in a T-shape configuration at different spacing.

### **1.6 LIMITATIONS OF THE STUDY**

- Results can vary with the different shape and configuration of the building.
- Building located in different zones can lead to different results.
- Different parameters like topography and other geographical conditions can cause influence on the building and the results may vary.

## **CHAPTER 2**

### **LITERATURE REVIEW**

#### **2.1 INTRODUCTION**

The purpose of this research is to understand how low-rise buildings behave and study the pressure distribution generated by wind over different types of roofs. It is necessary to pre-model aerodynamic conditions for the selected building in order to provide exactness in calculation of wind effect with the help of a wind tunnel.

There has been considerable research done on different methods of wind load distribution such as wind tunnel testing, computational fluid dynamics and codal provisions.

#### **2.2 LITERATURE REVIEW**

A hemispherical dome with varying aspect ratios is used in Taylor's study in order to determine local peak pressures and area-average pressures in turbulent shear flows. The crucial portions of a hemispherical dome have been discovered to be dependent on and responsive to wind direction [1].

According to Hoxey et al., the way wind pressure is distributed on a building is greatly influenced by the building's geometry. According to research conducted on building roofs, the pressure distribution is not uniform and varies with the building shape's geometrical characteristics as well as the roof's pitch and eave height [2].

According to Richards et al., the mean pressure coefficient distribution for the Silsoe cube agrees with both quantitative measurements and experimental results [3].

Experimental and numerical methods were used by Tvakol et al. to determine the mean surface pressure coefficients and velocity field in the airflow field around a surface-mounted hemisphere of a given height[4].

Using one layer space truss domes (with a constant span), Alireza and Mohammad studied the geometry of the domes. There was a linear relationship between wind pressure and the deformation of the low and high rise domes [5].

The primary objective of this study was, according to Yong et al., to evaluate the effects of surrounding structures and to investigate wind load prediction methodologies. This study revealed that proximity effects play a significant role in wind load estimation. As density increases, these effects become more prominent, resulting in the isolated model test not being able to adequately compensate [6].

Zhou et al. studied the effects of microburst-wind loads on low-rise buildings of different geometries, including a cube model, a grain bin model, and a model of a two-storey building with gables in a laboratory study. The flow patterns within the microburst-like wind were revealed using velocity and turbulence profiles [7].

In their experiment, Verma and Ahuja investigated low-rise buildings with domical roofs. A dome roof often experiences suction-like wind distribution [8].

Verma and Ahuja investigated rectangular-plan structures with multiple domes. Regardless of the number of domes, the wind pressure distribution and the pressure and suction values are nearly equal. There is approximately a comparable or greater value of suction on windward and leeward domes than on in-between domes [9].

A wind tunnel test model of a low-rise building with a circular cylinder roof and convex type roof was used by Verma and Ahuja to collect data on wind pressure distribution at various wind incidence angles. On the windward side of the roof, the most suction is observed near the apex[10].

In a uniform flow with little turbulence, Sadeghi et al. studied the effect of Reynolds number on wind loads on cylindrical roofs. The variable range of  $C_p$  depends on its aspect ratio, according to research [11].

A two-story building with a square shape and a pyramidal roof was investigated by Singh and Roy using ANSYS CFD, a powerful tool that produces graphical results. In this way, values such as pressure coefficients, velocity, pressure statics, dynamic pressure, and so on can be displayed on any plane, surface, or line efficiently [12].

The pressure coefficient values of the Euro code were compared to those of the CFD for dome by Nourhan et al. Domes' CFD values for the front and centre zones are very close to the applicable Euro Code values (around 5% difference)[13].

Ong et al. used CFD to analyze a building that is a low rise submerged in a boundary layer that is turbulent, and discovered that maximum pressure evaluation is essential for the design of the cladding[14].

Stathopoulos T. investigated the wind-induced pressure for an L-shaped low-rise model using a computational approach for normal wind direction. The findings of the computational and experimental studies were found to be comparable [15].

Kushal (2013) conducted experimental study on building model of T-shape and L-shape cross-section of aspect ratio 1:200. It was presented that pressure and force coefficient around the surface of high rise building model under isolated and interfering condition [16].

To determine drag shear and bracing loads in the direction corresponding to the frames parallel to the ridge, Gregory et al. performed wind tunnel studies on open-frame, low-rise buildings. In general, the worst wind angles were between  $0^\circ$  and  $40^\circ$ , with  $20^\circ$ – $30^\circ$  often having a higher load coefficient [17].

Singh and Roy simulated the variation in pressure due to wind load on a two-story building with a square plan and pyramidal roof using CFD. In order to achieve good

results and simplify the simulation process, a mesh quality of over 0.5 should be used and the mesh quality should be checked for each model [18].

Ahlawat and Ahuja conducted wind tunnel studies on a model of a T-shaped building to estimate wind loads and found that wind patterns around the building are heavily influenced by nearby buildings [19].

An experimental study by Ahlawat and Ahuja on a tall structure with a "Y" plan shape was conducted in a wind tunnel, and they found that wind incidence angle affects wind pressure distribution [20].

Raj and Ahuja discovered that the shear at the base, moments, and twisting moments are affected by wind incidence angle as well as by the cross-sectional shape in an experimental investigation of cross-shaped tall buildings[21].

Vafaeihosseini et al. while studying high-rise buildings with computational fluid dynamics, found rectangle shape plan shapes to be the most economical shapes in terms of wind load [22].

In a study by Meena et al. they discussed how the wind affected the bracing system used on steel buildings of different sizes [23].

The studies of Pal et al. examined the interference effects of square and fish plan shaped tall buildings for wind response, as well as the maximum efficiency pressure, as well as the base shear exhibited by a square plan shaped model under the given conditions of full blockage [24].

Verma et al. studied tall buildings of octagonal shape for wind induced response, using CFD simulation for wind incidence angle, and found that CFD can be used to predict wind-induced response on buildings as well as other types of structures.[25].

Wind effects of standard plan shape building and structures are provided in numerous international standards for example Australian code/New Zealand code AS/NZS 1170.2: 2011 [32], American code ASCE 7-16 [33], Indian standard code IS: 875 (Part-

3), 2015 [34]. Nevertheless, the given international codes fail to address the response of wind associated with distinctive or irregular shaped buildings. A regular building model generates critical pressure distribution mostly on windward faces, but distinctive or irregular plan shaped buildings can exhibit critical pressure distribution.

### **2.3 LITERATURE GAP**

- There has been no study reported till now for interference effects on multiple dome roof low-rise buildings arranged in a specific shape or configuration.
- There has been no study how building placed at different distances effect the wind load distribution of structures.
- The codal provision of IS 875 (part 3) limits the coefficient of pressure  $C_p$  values to 0 and 90 degree wind incidence angles, and to standard-shaped buildings only.

## **CHAPTER 3**

### **VALIDATION**

#### **3.1 GENERAL**

To start off the detailed numerical analysis of different models, we need to confirm that flow conditions and results from ANSYS CFX package are valid. To do this, we analyze model by Astha Verma's, Ashok K. Ahuja of research paper Wind Pressure Distribution on Domical Roofs International Journal of Engineering and Applied Sciences (IJEAS) ISSN: 2394-3661, Volume-2, Issue-5, and May 2015. The IS code 875 part 3 calculated wind pressure distribution for domical roofs is also compared with our results from ANSYS CFX package.

#### **3.2 DETAILS OF MODEL**

The square building block has a plan dimension of 254 mm by 254 mm, and height of 150mm. Domes have diameters of 254 mm and heights 84 mm. A scale 1:50 is used for creating the model in this project. The Wind tunnel dimension is taken as per the specifications 4680 mm\*2340 mm\*1404 mm.



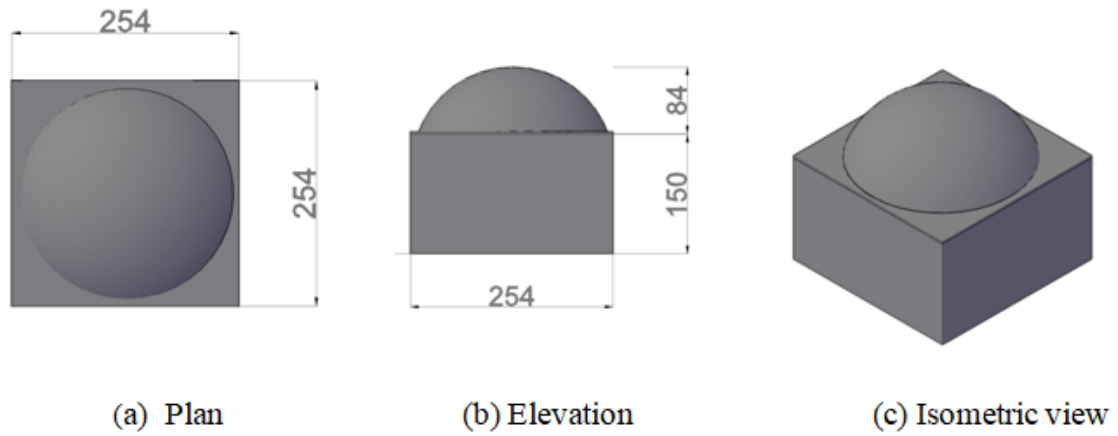


**Fig 3.1 Dimensions of the Validation model in mm**

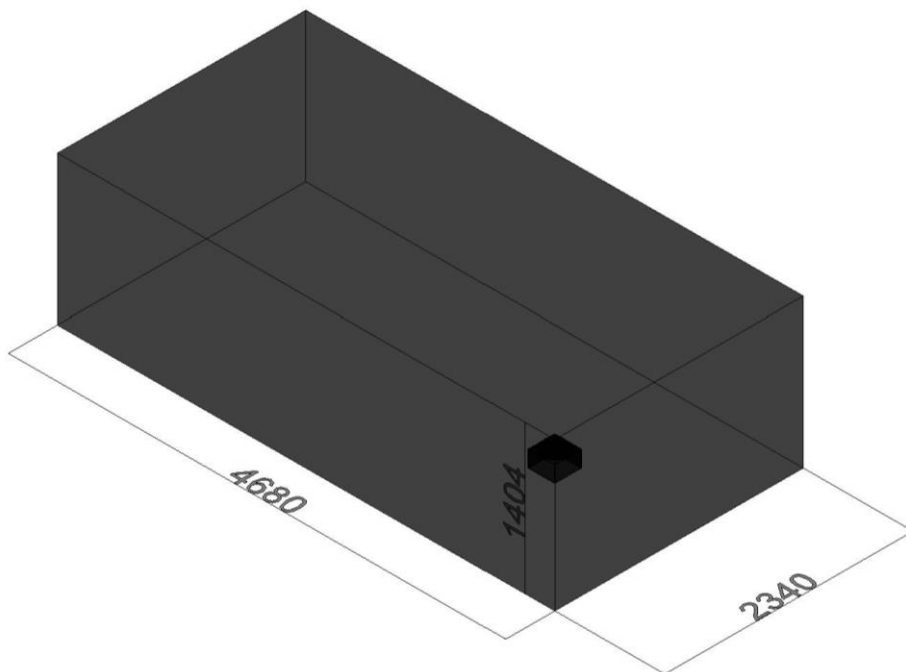


**Fig 3. 2 Computational domain used for CFD simulation (dimensions in mm)**

### 3.3 NUMERICAL ANALYSIS

A steady state analysis was done for the simulation in order to build a model of SST turbulence. The SST model combines the accuracy and resilience of the standard  $k$ - $\omega$  model in the near-wall area with the free stream insensitivity of the standard  $k$ - $\varepsilon$  model in a modified formulation distant from the wall through a blending function[26][27]. Furthermore, the turbulent shear stress transfer is incorporated in the turbulent viscosity formulation to enhance predictions of the flow separation initiation for flows on smooth surfaces with unfavourable pressure gradients, such as flows over airfoils.

The SST model is a reliable two-equation eddy-viscosity turbulence model that is widely utilised.

K- $\omega$  SST model of Menter's can be summarized as follows[31]:

$$\frac{\partial(\partial k)}{\partial t} + \frac{\partial(\rho U_j k)}{\partial x_j} = \frac{\partial}{\partial x_j} \left[ \left( \mu + \frac{\mu_t}{\sigma_k} \right) \frac{\partial k}{\partial x_j} \right] + P - \beta \rho k \omega$$

$$\frac{\partial(\rho \omega)}{\partial t} + \frac{\partial(\rho U_j \omega)}{\partial x_j} = \frac{\partial}{\partial x_j} \left[ \left( \mu + \frac{\mu_t}{\sigma_\omega} \right) \frac{\partial \omega}{\partial x_j} \right] + \alpha \frac{\omega}{k} P - \beta \rho \omega^2 + 2(1 - F_1) \frac{\rho \sigma \omega_2}{\omega} \frac{\partial k}{\partial x_j} \frac{\partial \omega}{\partial x_j}$$

$2(1 - F_1) \frac{\rho \sigma \omega_2}{\omega} \frac{\partial k}{\partial x_j} \frac{\partial \omega}{\partial x_j}$  is the Cross diffusion term and F1 is the blending function.

At the boundary layer depth, the inlet wind velocity is 10 m/s. The relative pressure of the outflow used is, 0 Pa. The domain's working pressure is taken as 1 atm. The tetrahedral meshing method is used to mesh the domain [28][29] .

For the results , gridlines were defined for the dome using point cloud in ANSYS so as to find pressure values at the respective grids and the results were extracted in the excel file.

The external pressure coefficient 'Cp' is calculated using the formula in the excel

$$C_p = \frac{P}{\frac{1}{2} \rho v^2}$$

where P is the actual wind pressure,  $\rho$  is the density of air and v is the reference velocity at building height.

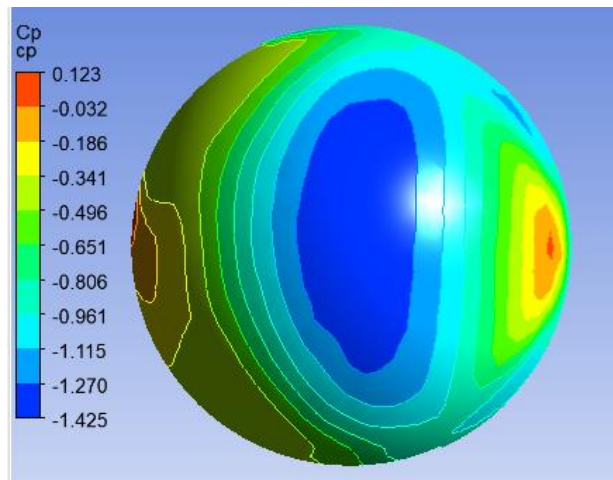


**Fig 3.3 Cp contours for the validation model**

The results of ANSYS as shown in Fig 3.3 are compared with External pressure values of curved roof as per IS 875 part 3 (2015) clause 7.3.3.6.

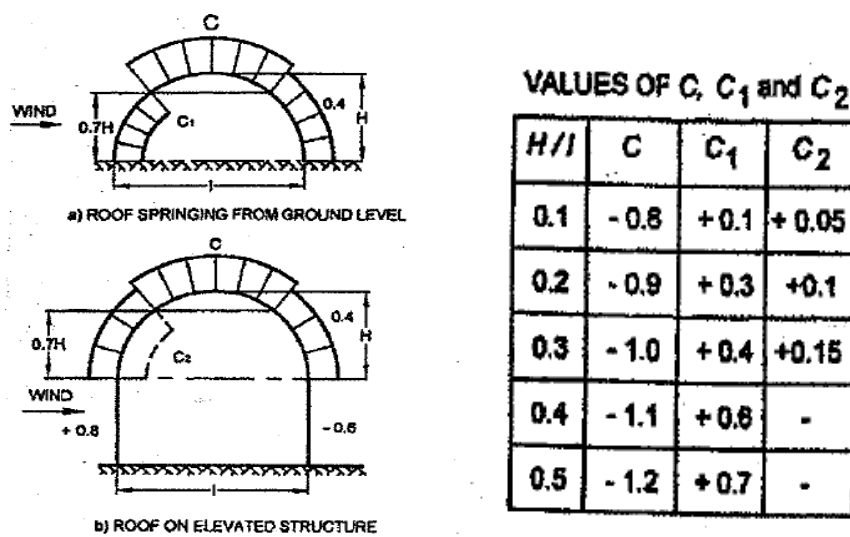


**Fig 3.4 Cp values of curved roof as per IS 875 Part 3 (2015) clause 7.3.3.6**

### 3.4 RESULTS

**Table 3.1 Comparative study of results from ANSYS CFX and IS code 875 Part 3**

Face	Values of Cp obtained from CFD analysis	Values of Cp as per IS 875 part III (2015)	Percentage of error %
Windward face	0.123	0.150	18
Top	-1.084	-1.050	2.85
Leeward face	0.432	0.40	8

The results of the ANSYS CFX package are validated with the values of Coefficient of pressure from IS code provisions 875 part 3 (2015) and the percentage error on average is found to be 9.61%.

Hence, the results of ANSYS is validated with IS code provisions.

## **CHAPTER 4**

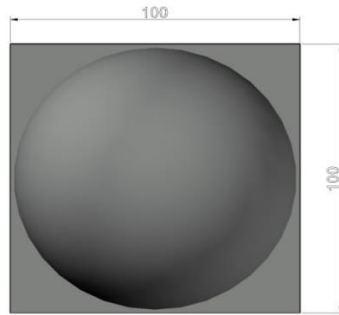
### **WIND RESPONSE ANALYSIS**

#### **4.1 GENERAL**

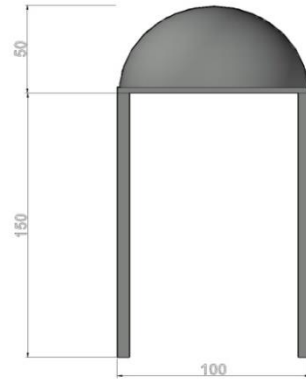
As per description of chapter 1 to carry out the CFD analysis of low rise building with domical roof was mentioned, we have used ANSYS software for the simulation of the natural wind flow for the low rise building. The purpose of this numerical study was to carry out extensive wind tunnel testing on rigid model of the isolated low rise building and building arranged in different configuration at different spacing's to evaluate pressure phases of the building models and to find out the coefficient of pressure and velocity streamlines.

#### **4.2 DETAILS OF MODEL**

The model of the isolated building is square in plan with dimensions of 100 mm by 100mm in length and width and the elevation of the domical roof is taken as 50 mm, with a total height of 200 mm. Fig 4.1 shows the front and top views of the isolated building model. A model is created by arrangement of five domical low-rise buildings in a T-shape at different spacing (0,  $b/2$ ,  $b$ , and  $3b/2$ ,  $2b$ ) between them where  $b$  is the width of the isolated dome as shown in the figure Fig 4.2 to Fig 4.6. A second model is created by arrangement of four domical low-rise buildings in a L-shape at different spacing (0,  $b/2$ ,  $b$ ,  $3b/2$ ,  $2b$ ) between them where  $b$  is the width of the isolated dome as shown in the Fig 4.7 to Fig 4.11.

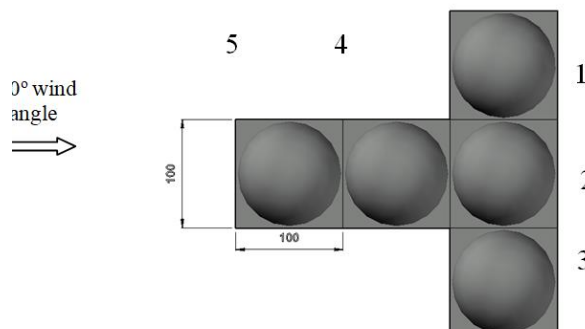


(a) Plan

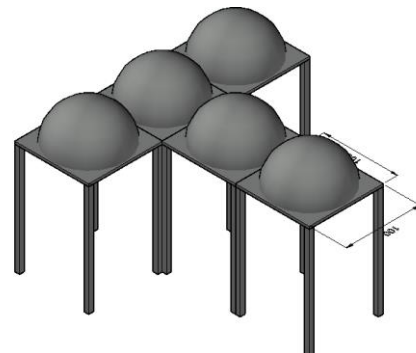


(b) Elevation

**Fig 4. 1 Dimensions of the isolated building model in mm**

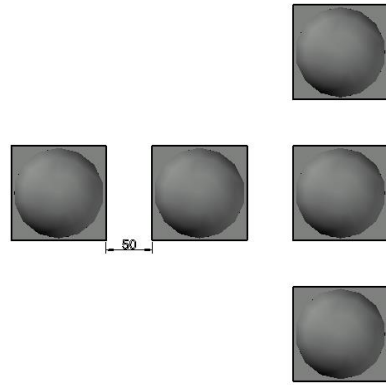


(a) Plan

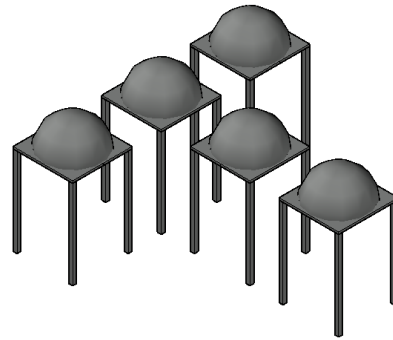


(b) Isometric view

**Fig 4. 2 Plan and Isometric view of arrangement of domical roof buildings in T shape at 0 mm spacing**

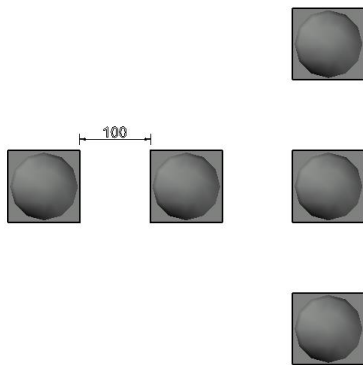


(a) Plan

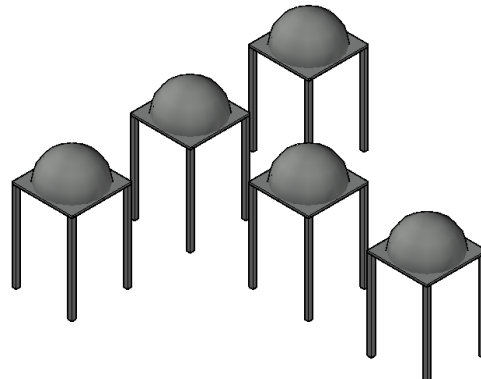


(b) Isometric view

**Fig 4. 3 Plan and Isometric view of arrangement of domical roof buildings in T shape at 50 mm spacing**



(a) Plan



(b) Isometric view

**Fig 4. 4 Plan and Isometric view of arrangement of domical roof buildings in T shape at 100 mm spacing**

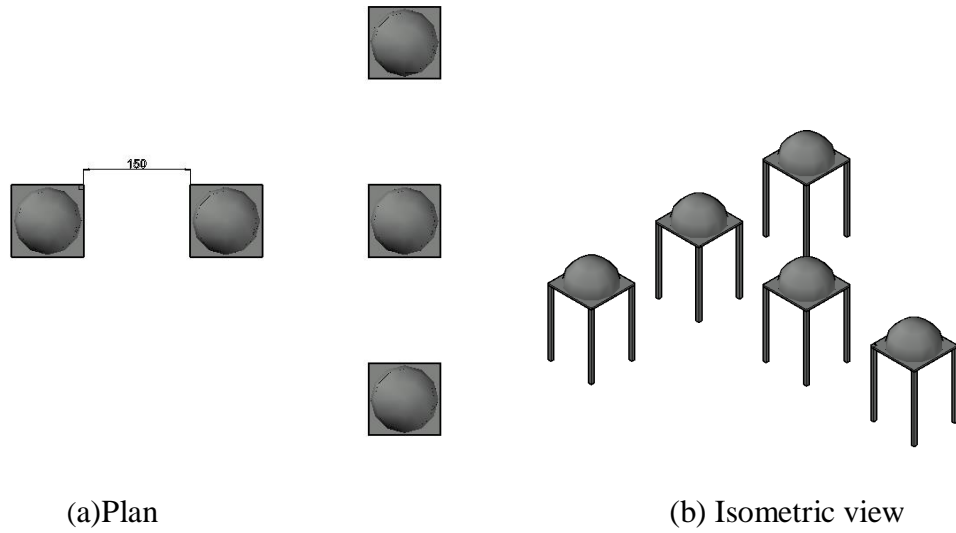


**Fig 4. 5 Plan and Isometric view of arrangement of domical roof buildings in T shape at 150 mm spacing**

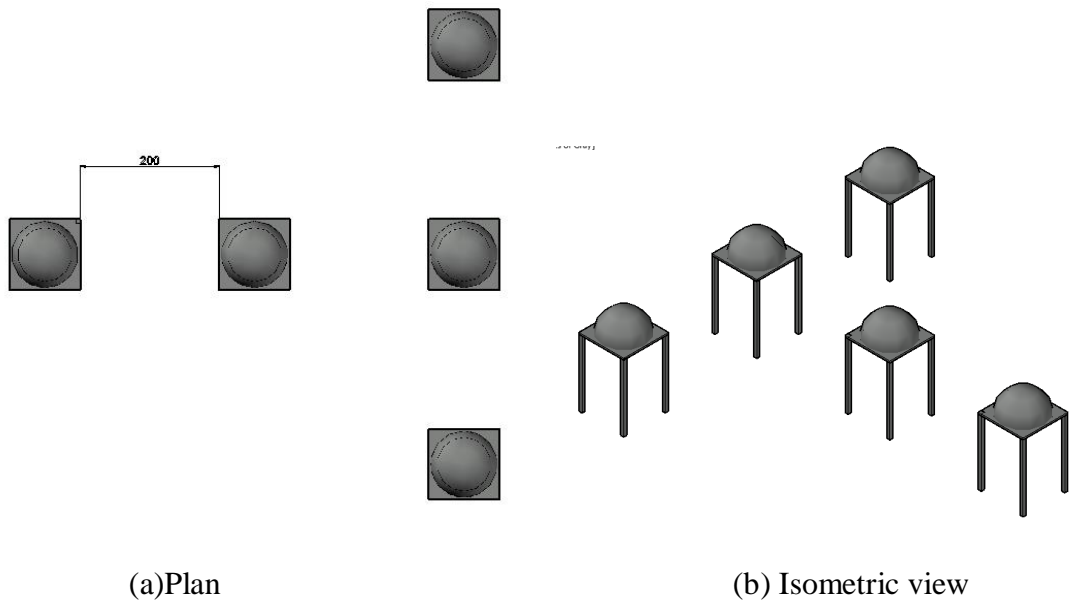


**Fig 4. 6 Plan and Isometric view of arrangement of domical roof buildings in T shape at 200 mm spacing**



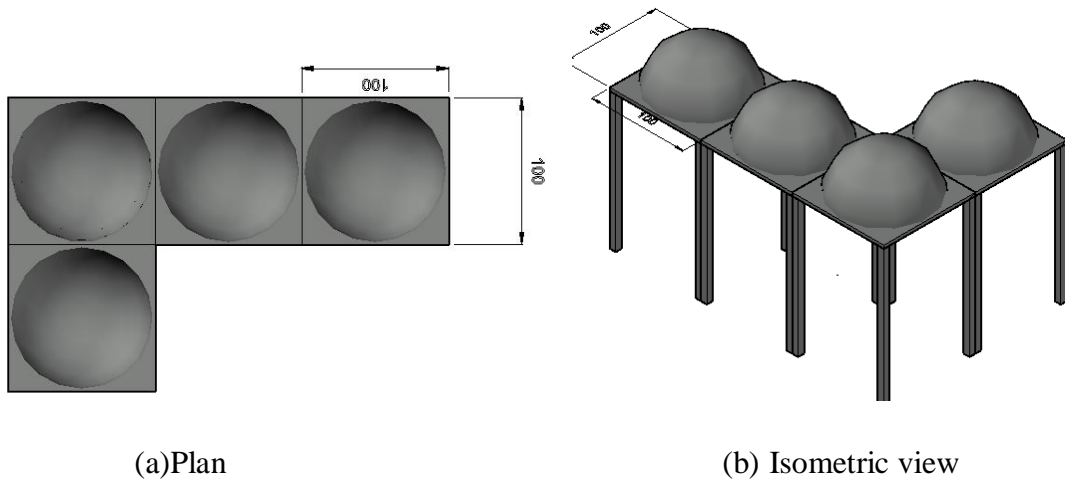


**Fig 4. 7 Plan and Isometric view of arrangement of domical roof buildings in L shape at 0 mm spacing**

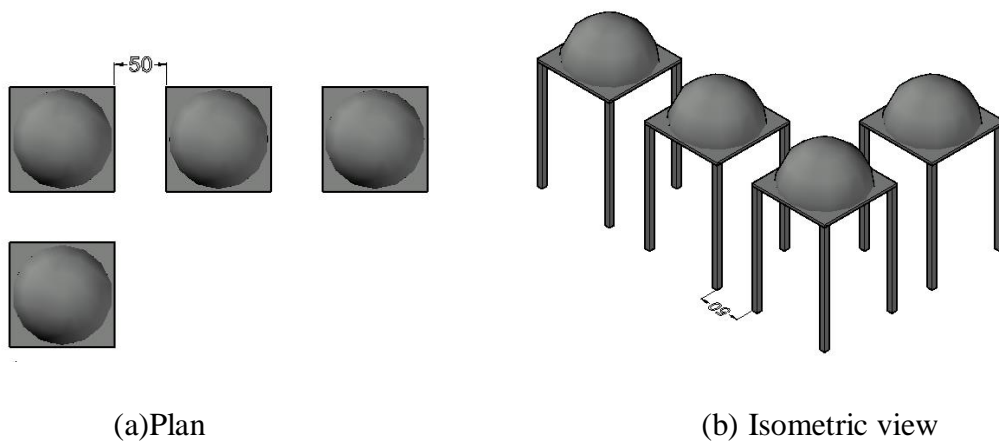
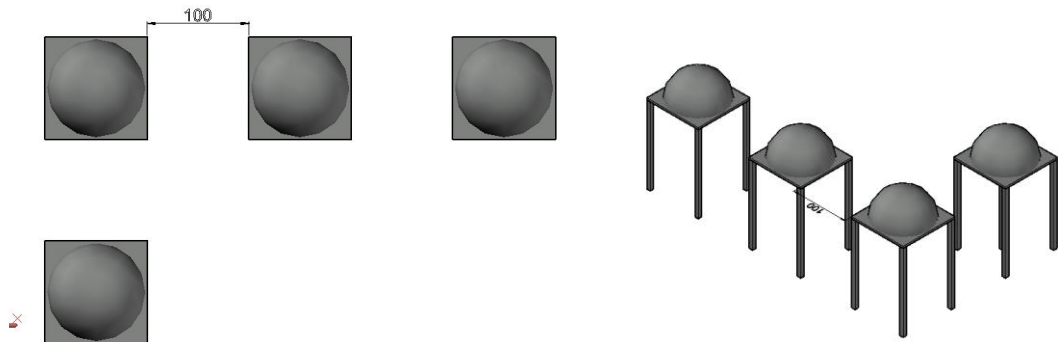


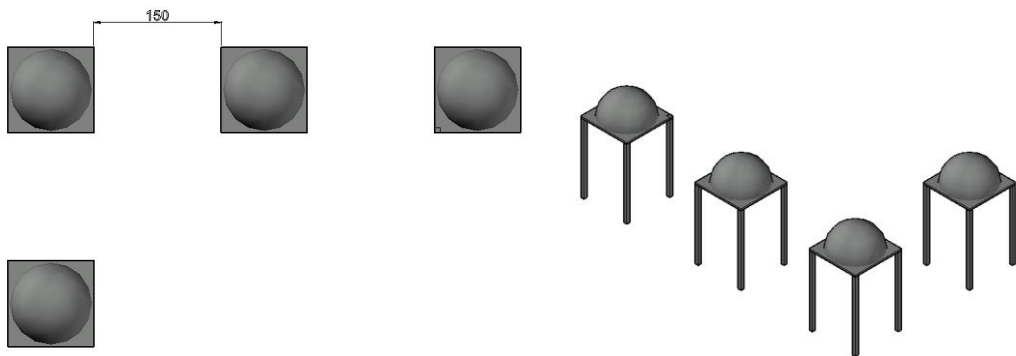
**Fig 4. 8 Plan and Isometric view of arrangement of domical roof buildings in L shape at 50 mm spacing**



(a)Plan

(b) Isometric view

**Fig 4. 9 Plan and Isometric view of arrangement of domical roof buildings in L shape at 100 mm spacing**



(a)Plan

(b) Isometric view

**Fig 4. 10 Plan and Isometric view of arrangement of domical roof buildings in L shape at 150 mm spacing**

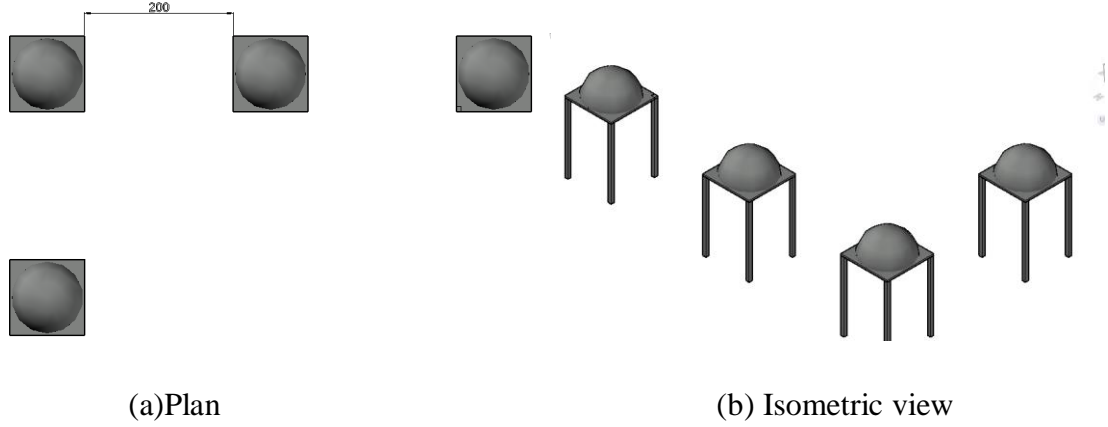


**Fig 4. 11 Plan and Isometric view of arrangement of domical roof buildings in L shape at 200 mm spacing**

The domain is represented at a scale factor of 1:50, with a wind velocity of 10 m/s at the inlet. The steady state analysis is carried out, and the numerical simulation is carried out using the SST turbulence model. The given model is a hybrid of the  $k-\omega$  and  $k-\epsilon$  turbulence models, reads velocity flow on the near wall zone of a bluff body as well as the far wall region. In this type of flow problem, the SST model may be the optimum option.

### 4.3 DETAILS OF WIND TUNNEL

#### 4.3.1 COMPUTATIONAL DOMAIN

The recommendation of [28] is strictly adhered to while selecting the domain size [Fig.7]. The domain of the model is  $20H$  length,  $10H$  width and  $5H$  height, with  $H$  is the height that matches the top of the building. This size allows enough time for vortices to form properly and avoids block flow caused by wind. Blockage removal is also non-mandatory. The domain is meshed using a tetrahedral type of meshing [29][30][Fig. 4.13]. Tetrahedral elements could also be used for arbitrary geometries with high accuracy, as well as those that are structurally tetrahedral. A simple cubic grid applied in 3D or a square grid applied in 2D would yield less accurate results than one composed of tetrahedrons. Tetrahedrons are typically positioned where highly precise flow is required, such as near the edges of system boundaries where curved surfaces

exist. Hexahedrons may be ideal for modelling wall-bounded flows, symmetric surfaces, or large flat areas, as complex flows are unlikely to occur there.

The effect of wind on the building model is investigated using CFD simulation. CFD works by splitting the location into a grid of many cells. The cell grid is surrounded by a space that simulates an opening and a surface that surrounds the boundary. The restraint pressure, and the movement of the air in the opening in the cell, is then adjusted to an initial state close to the actual environment of the wind tunnel experiment. The side panels and ceiling remain in front of the CFX as free slips. During this investigation, the floor surface and building model will be treated as non-slip walls within the pre CFX configuration. No-slip means that the velocity of air at the boundary of the wall is the same as the velocity of air at the inlet. The value of the velocity parallel to the wall is finite (calculated by the solver), but both the velocity perpendicular to the wall and the shear stress are set to zero. For effective wind component capture, finer meshing is provided near the structure and faces of domain. To provide continuous flow at the separating locations, mesh inflation is done along the boundaries.

In our investigation, the simulation and grid are developed at a smaller scale (1:50). The building model and the computational domain in Fig 4.12 follow the best practise recommendations established by Franke et al. [34] and Revuz et al. [15]. The dimensions of the domain are 4000mm×2000mm×1000 mm (W×D×H) which correspond to 200m×100m×50 m in full scale.

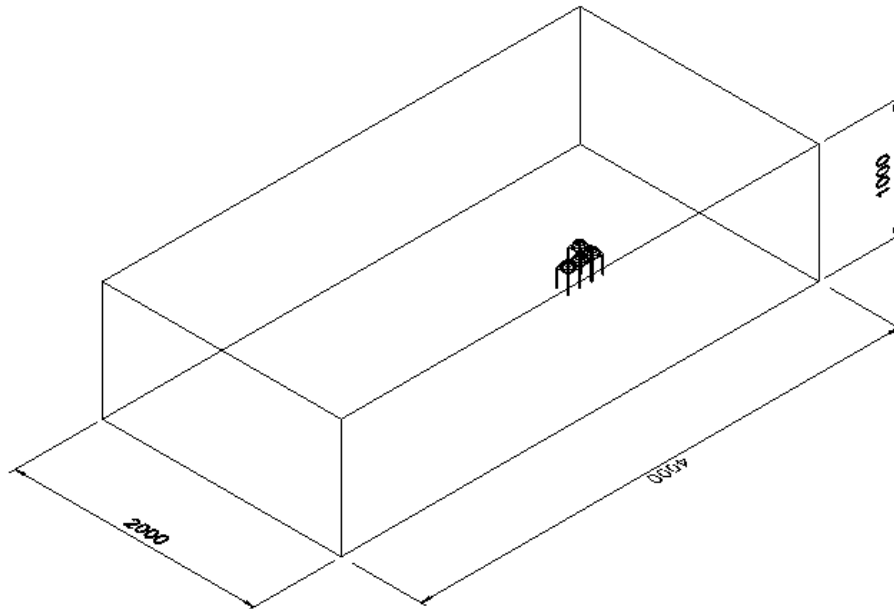


**Fig 4. 12 Model and the computational domain used for simulation in ANSYS  
(dimensions in mm)**

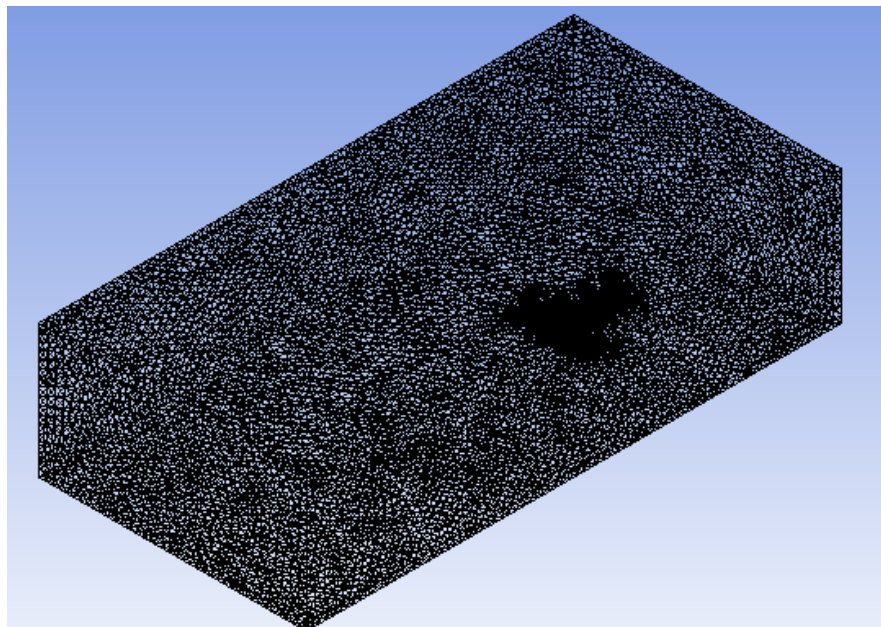


**Fig 4.13 Tetrahedral meshing used for CFD simulation**

#### 4.4 SHEAR STRESS TRANSPORT MODEL

A steady state analysis was done for the simulation in order to build a model of SST turbulence. The SST model combines the accuracy and resilience of the standard  $k$ - $\omega$  model in the near-wall area with the free stream insensitivity of the standard  $k$ - $\varepsilon$  model in a modified formulation distant from the wall through a blending function[26][27]. Furthermore, the turbulent shear stress transfer is incorporated in the turbulent viscosity formulation to enhance predictions of the flow separation initiation for flows on smooth surfaces with unfavourable pressure gradients, such as flows over airfoils.

The SST model is a reliable two-equation eddy-viscosity turbulence model that is widely utilised.

$k$ - $\omega$  SST model of Menter's can be summarized as follows[31]:

$$\frac{\partial(\rho k)}{\partial t} + \frac{\partial(\rho U_j k)}{\partial x_j} = \frac{\partial}{\partial x_j} \left[ \left( \mu + \frac{\mu_t}{\sigma_k} \right) \frac{\partial k}{\partial x_j} \right] + P - \beta \rho k \omega$$

$$\frac{\partial(\rho \omega)}{\partial t} + \frac{\partial(\rho U_j \omega)}{\partial x_j} = \frac{\partial}{\partial x_j} \left[ \left( \mu + \frac{\mu_t}{\sigma_\omega} \right) \frac{\partial \omega}{\partial x_j} \right] + \alpha \frac{\omega}{k} P - \beta \rho \omega^2 + 2(1 - F_1) \frac{\rho \sigma \omega_2}{\omega} \frac{\partial k}{\partial x_j} \frac{\partial \omega}{\partial x_j}$$

$2(1 - F_1) \frac{\rho \sigma \omega_2}{\omega} \frac{\partial k}{\partial x_j} \frac{\partial \omega}{\partial x_j}$  is the Cross diffusion term and  $F_1$  is the blending function.

At the boundary layer depth, the inlet wind velocity is 10 m/s. The relative pressure of the outflow used is, 0 Pa. The domain's working pressure is taken as 1 atm. The tetrahedral meshing method is used to mesh the domain [28][29] .

## **CHAPTER 5**

### **RESULTS**

#### **5.1 GENERAL**

Result of Coefficient of pressure, and streamlines for isolated, T shape domical building and L shape domical building placed at different distances is presented by pictorial and tabular representation in various plots in the following sections.

#### **5.2 ISOLATED BUILDING**

##### **5.2.1 COEFFICIENT OF PRESSURE ( $C_p$ )**

The wind pressure coefficient ( $C_p$ ) in buildings is one of the most important quantities used in many disciplines of building engineering's, such as load calculations, ventilation, and structural design. A dimensionless quantity known as  $C_p$  represents the relationship between the wind velocity and pressure generated at the building's surface. After considering the geographical location, terrain conditions and shielding effect, the static and design wind pressure are measured at the height of the point considered.

For the isolated building, the pressure on the windward face is positive for the domical roof. It is negative for the apex of the dome roof, as seen in Fig 5.1 depicts the pictorial representation of pressure on each face of the isolated building, with the maximum negative pressure in the centre of the dome and decreasing in the corner region. The rest of domical roof is under the influence of positive pressure, as shown in Fig 5.1. Pressure decreases along the wind direction up to the apex of the dome due to the suction created, and after that it starts increasing again along the direction of the wind.

The maximum coefficient of pressure  $C_p$  was found to be on the windward side with the magnitude of 1.050 and on the apex of the dome the maximum negative value of  $C_p$

was obtained with the magnitude of -1.242 and on the leeward side the dome was in the influence of very low positive pressure and the  $C_p$  was found to be 0.363 as shown in Fig 5.2.

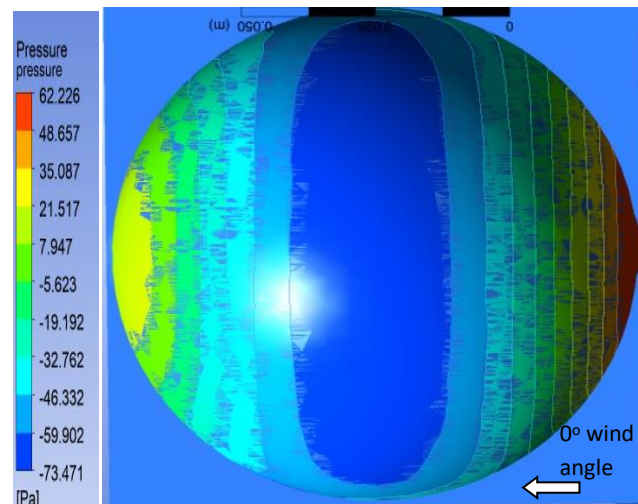


**Fig 5. 1 Pressure contours on the isolated building**

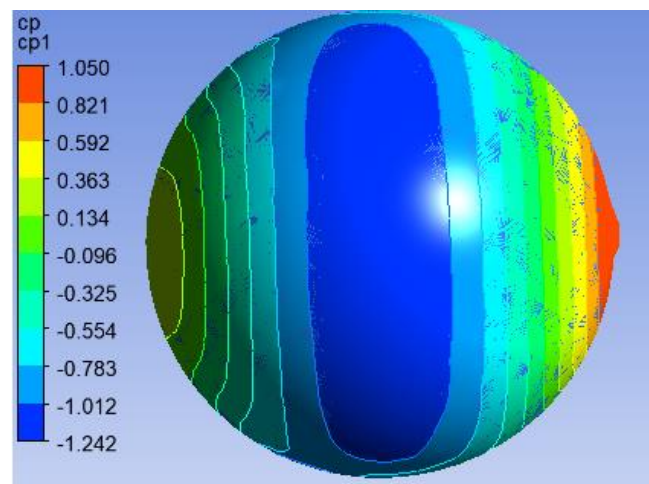


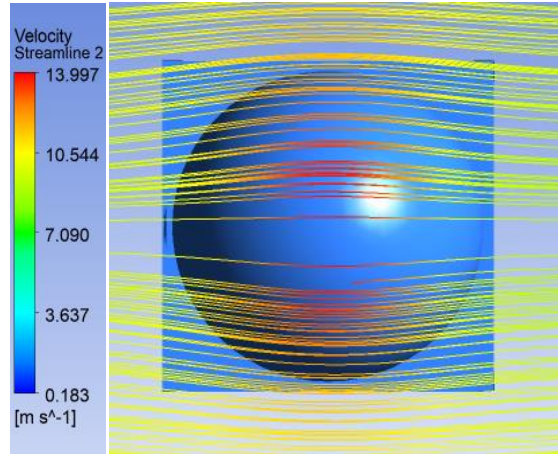
**Fig 5. 2  $C_p$  contours for the isolated building model**



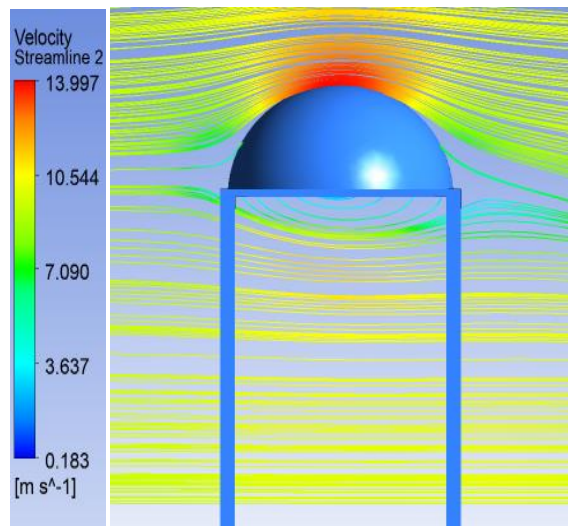
### 5.2.2 VELOCITY STREAMLINES

A streamline in a fluid is an imaginary line whose tangent at any point depicts the direction of a fluid particle's velocity at that position. Streamlines are the fluid flow directions, around bodies and in channels, It indicates what the flow conditions are, laminar, turbulent or separated. It indicates what is going on and where corrections are needed. Because various flow patterns are observed for buildings, and it is due to the variation in the plan shape of the building, it is necessary to observe for velocity streamlines in order to determine behaviour of wind surrounding the building.

In the wake zone, vortices are generated on the downstream side of building model for isolated building which has a large recirculation zone of air. There is a separation of the flow along the leading edges of the roofs and sides of the building and those separated layers move into the surrounding fluid. These layers will eventually converge on the wake axis, leading to a relatively imprecisely defined area known as a cavity. The streamlines emanating from the corners frame the cavity laterally as well. For a  $0^\circ$  wind incidence angle, the streamline is depicted in Fig. 7 in plan and Fig. 8 in elevation. This colour scale shows the velocity of streamlines, which is higher on the windward side than on the leeward side.



(a) Top View



(b) Front view

**Fig 5. 3 Velocity Streamlines for isolated building model**

### 5.3 BUILDING ARRANGED IN T- SHAPE CONFIGURATION

For the arrangement of building arranged in T shape configuration, the wind incidence angle is varied from  $0^\circ$  to  $180^\circ$  at an interval of 30 degree as there is symmetry of the building and the spacing between the building is varied at a distance of 0,  $b/2$ ,  $b$ ,  $3b/2$  and  $2b$  where  $b$  is the width of the isolated building i.e. 0mm, 50mm, 100mm, 150mm and 200mm.

#### 5.3.1 COEFFICIENT OF PRESSURE ( $C_p$ )

- For 0 mm spacing

**Table 5. 1 Coefficient of pressure ( $C_p$ ) for T shape configuration at 0 mm spacing**

$C_p$					
WIA	DOME 1	DOME 2	DOME 3	DOME 4	DOME 5
$0^\circ$	-0.48797	-0.28416	-0.49163	-0.05174	-0.15711
$30^\circ$	-0.32098	-0.37554	-0.52536	-0.2026	-0.28027
$60^\circ$	-0.2559	-0.41512	-0.37246	-0.53934	-0.49015
$90^\circ$	-0.20733	-0.2349	-0.13477	-0.50622	-0.53724
$120^\circ$	-0.5382	-0.29779	-0.16417	-0.44844	-0.55937
$150^\circ$	-0.61294	-0.46923	-0.41207	-0.22178	-0.4229
$180^\circ$	-0.42504	-0.40378	-0.46947	-0.13601	-0.14846

It was observed that for 0 mm spacing between the buildings when arranged in T shape configuration the average coefficient of pressure value is found to be negative i.e. suction is acting on the surface of domes.

When the wind angle is varied from  $0^\circ$  to  $180^\circ$  it is observed that for dome 1 the largest magnitude peak negative of Coefficient of pressure  $C_p$  is -0.61294 for  $150^\circ$  wind incidence angle, for dome 2 the largest magnitude peak negative of Coefficient of pressure  $C_p$  is -0.46923 for  $150^\circ$  wind incidence angle, for dome 3 the largest magnitude peak negative of Coefficient of pressure  $C_p$  is -0.52536 for  $30^\circ$  wind

incidence angle ,for dome 4  $C_p$  is found to be -0.53934 for  $60^\circ$  wind incidence angle and for dome 5  $C_p$  is found to be -0.55937 for  $120^\circ$  wind incidence angle.

- **For 50 mm spacing**

**Table 5. 2 Coefficient of pressure ( $C_p$ ) for T shape configuration at 50 mm spacing**

$C_p$					
WIA	DOME 1	DOME 2	DOME 3	DOME 4	DOME 5
$0^\circ$	-0.47625	-0.31924	-0.49259	-0.17212	-0.26242
$30^\circ$	-0.3717	-0.51848	-0.48131	-0.36952	-0.37212
$60^\circ$	-0.40195	-0.46191	-0.40767	-0.46861	-0.42759
$90^\circ$	-0.28432	-0.25058	-0.31887	-0.52123	-0.49035
$120^\circ$	-0.48065	-0.37044	-0.34122	-0.38784	-0.49371
$150^\circ$	-0.51059	-0.42856	-0.41033	-0.32062	-0.36851
$180^\circ$	-0.44562	-0.3648	-0.44155	-0.21159	-0.26463

It was observed that for 0 mm spacing between the buildings when arranged in T shape configuration the average coefficient of pressure value is found to be negative i.e. suction is acting on the surface of domes and the negative  $C_p$  value was found to be reduced by 6.27 % in comparison to values of  $C_p$  for 0 mm spacing.

When the wind angle is varied from  $0^\circ$  to  $180^\circ$  it is observed that for dome 1 the largest magnitude peak negative of Coefficient of pressure  $C_p$  is -0.51059 for  $150^\circ$  wind incidence angle , for dome 2 the largest magnitude peak negative of Coefficient of pressure  $C_p$  is -0.51848 for  $30^\circ$  wind incidence angle , for dome 3 the largest magnitude peak negative of Coefficient of pressure  $C_p$  is -0.49259 for  $0^\circ$  wind incidence angle ,for dome 4  $C_p$  is found to be -0.52123 for  $90^\circ$  wind incidence angle and for dome 5  $C_p$  is found to be -0.49371 for  $120^\circ$  wind incidence angle.

- For 100 mm spacing

**Table 5. 3 Coefficient of pressure (Cp) for T shape configuration at 100 mm spacing**

Cp					
WIA	DOME 1	DOME 2	DOME 3	DOME 4	DOME 5
0°	-0.46952	-0.34688	-0.45825	-0.28484	-0.35177
30°	-0.39021	-0.47439	-0.44482	-0.39662	-0.4054
60°	-0.39745	-0.43577	-0.40348	-0.43995	-0.42706
90°	-0.32256	-0.30136	-0.33812	-0.44566	-0.45586
120°	-0.45962	-0.39675	-0.38132	-0.43275	-0.45626
150°	-0.42032	-0.37466	-0.35354	-0.34507	-0.34493
180°	-0.43561	-0.38639	-0.43562	-0.30752	-0.31419

It was observed that for 0 mm spacing between the buildings when arranged in T shape configuration the average coefficient of pressure value is found to be negative i.e. suction is acting on the surface of domes and the negative Cp value was found to be reduced by 10.61 % in comparison to values of Cp for 0 mm spacing.

When the wind angle is varied from 0° to 180° it is observed that for dome 1 the largest magnitude peak negative of Coefficient of pressure Cp is -0.46952 for 0° wind incidence angle , for dome 2 the largest magnitude peak negative of Coefficient of pressure Cp is -0.47439 for 30° wind incidence angle , for dome 3 the largest magnitude peak negative of Coefficient of pressure Cp is -0.45825 for 0° wind incidence angle ,for dome 4 Cp is found to be -0.44566 for 90° wind incidence angle and for dome 5 Cp is found to be -0.45626 for 120° wind incidence angle.

- For 150 mm spacing

**Table 5. 4 Coefficient of pressure (Cp) for T shape configuration at 150 mm spacing**

Cp					
WIA	DOME 1	DOME 2	DOME 3	DOME 4	DOME 5
0°	-0.46926	-0.37124	-0.4651	-0.32715	-0.39395
30°	-0.40705	-0.49419	-0.46086	-0.4152	-0.43233
60°	-0.44803	-0.47033	-0.41893	-0.46068	-0.46027
90°	-0.34443	-0.34295	-0.37814	-0.4521	-0.40315
120°	-0.46132	-0.44786	-0.42382	-0.46084	-0.48052
150°	-0.47449	-0.44245	-0.4316	-0.426	-0.43993
180°	-0.42482	-0.42603	-0.43146	-0.35769	-0.36726

It was observed that for 0 mm spacing between the buildings when arranged in T shape configuration the average coefficient of pressure value is found to be negative i.e. suction is acting on the surface of domes and the negative Cp value was found to be reduced by 12.24 % in comparison to values of Cp for 0 mm spacing

When the wind angle is varied from 0° to 180° it is observed that for dome 1 the largest magnitude peak negative of Coefficient of pressure Cp is -0.47449 for 150° wind incidence angle , for dome 2 the largest magnitude peak negative of Coefficient of pressure Cp is -0.49419 for 30° wind incidence angle , for dome 3 the largest magnitude peak negative of Coefficient of pressure Cp is -0.46084 for 120° wind incidence angle ,for dome 4 Cp is found to be -0.46084 for 120° wind incidence angle and for dome 5 Cp is found to be -0.48052 for 120° wind incidence angle.

- For 200 mm spacing

**Table 5. 5 Coefficient of pressure (Cp) for T shape configuration at 200 mm spacing**

Cp					
WIA	DOME 1	DOME 2	DOME 3	DOME 4	DOME 5
0°	-0.45681	-0.40847	-0.44956	-0.3555	-0.41338
30°	-0.43475	-0.49159	-0.4826	-0.44221	-0.44679
60°	-0.48695	-0.46263	-0.45151	-0.46059	-0.45595
90°	-0.3684	-0.36512	-0.40582	-0.4304	-0.43024
120°	-0.48551	-0.46615	-0.41343	-0.47583	-0.4764
150°	-0.4711	-0.45665	-0.465	-0.47389	-0.44512
180°	-0.4442	-0.42638	-0.438	-0.36694	-0.37966

It was observed that for 0 mm spacing between the buildings when arranged in T shape configuration the average coefficient of pressure value is found to be negative i.e. suction is acting on the surface of domes and the negative Cp value was found to be reduced by 14.52 % in comparison to values of Cp for 0 mm spacing

When the wind angle is varied from 0° to 180° it is observed that for dome 1 the largest magnitude peak negative of Coefficient of pressure Cp is -0.48695 for 60° wind incidence angle , for dome 2 the largest magnitude peak negative of Coefficient of pressure Cp is -0.49159 for 30° wind incidence angle , for dome 3 the largest magnitude peak negative of Coefficient of pressure Cp is -0.4826 for 30° wind incidence angle ,for dome 4 Cp is found to be -0.47583 for 120° wind incidence angle and for dome 5 Cp is found to be -0.4764 for 120° wind incidence angle.

### 5.3.2 VELOCITY STREAMLINES

A streamline in a fluid is an imaginary line whose tangent at any point depicts the direction of a fluid particle's velocity at that position. Streamlines are the fluid flow directions, around bodies and in channels, it indicates what the flow conditions are, laminar, turbulent or separated. It indicates what is going on and where corrections are needed. Because various flow patterns are observed for buildings, and it is due to the variation in the plan shape of the building, it is necessary to observe for velocity streamlines in order to determine behaviour of wind surrounding the building.

The wind flow streamlines for the arrangement of T shape model for different spacing's from 0 mm to 200 mm model are presented in the Fig 5.4 to Fig 5.8 respectively.

We can clearly see from the figures shown below that the streamlines vary with the wind incidence angle which signifies that the pressure distribution due to wind load is highly affected by certain factors on the roof of low-rise building are wind characteristics such as vortex, flow separation, stagnation, flow recirculation and flow reattachment.

It can be observed that the flow separates at the outer edge of the roofs and sides of the buildings, and the split layers of fluid move into the surrounding fluid. When the spacing is increased for the buildings, these layers may be able to rejoin to the surface. As a result, the separation is repeated at the roof's and sides' downwind borders. These layers are found to eventually converge on the wake axis, resulting in a very imprecisely defined area known as a cavity, regardless of how long or short the building is. The separating streamline emerges from the roof edge on the upwind and above sides. The reattachment streamline runs from the roof edge on the downwind side. Separating streamlines are not the same as reattachment streamlines in two-dimensional flows. The streamlines that emanate from the corners also serve to frame the hollow laterally. It can be seen that the flow inside this roughly ellipsoidal cavity has extremely high turbulence intensity and a low mean velocity, and it regularly reverses direction.



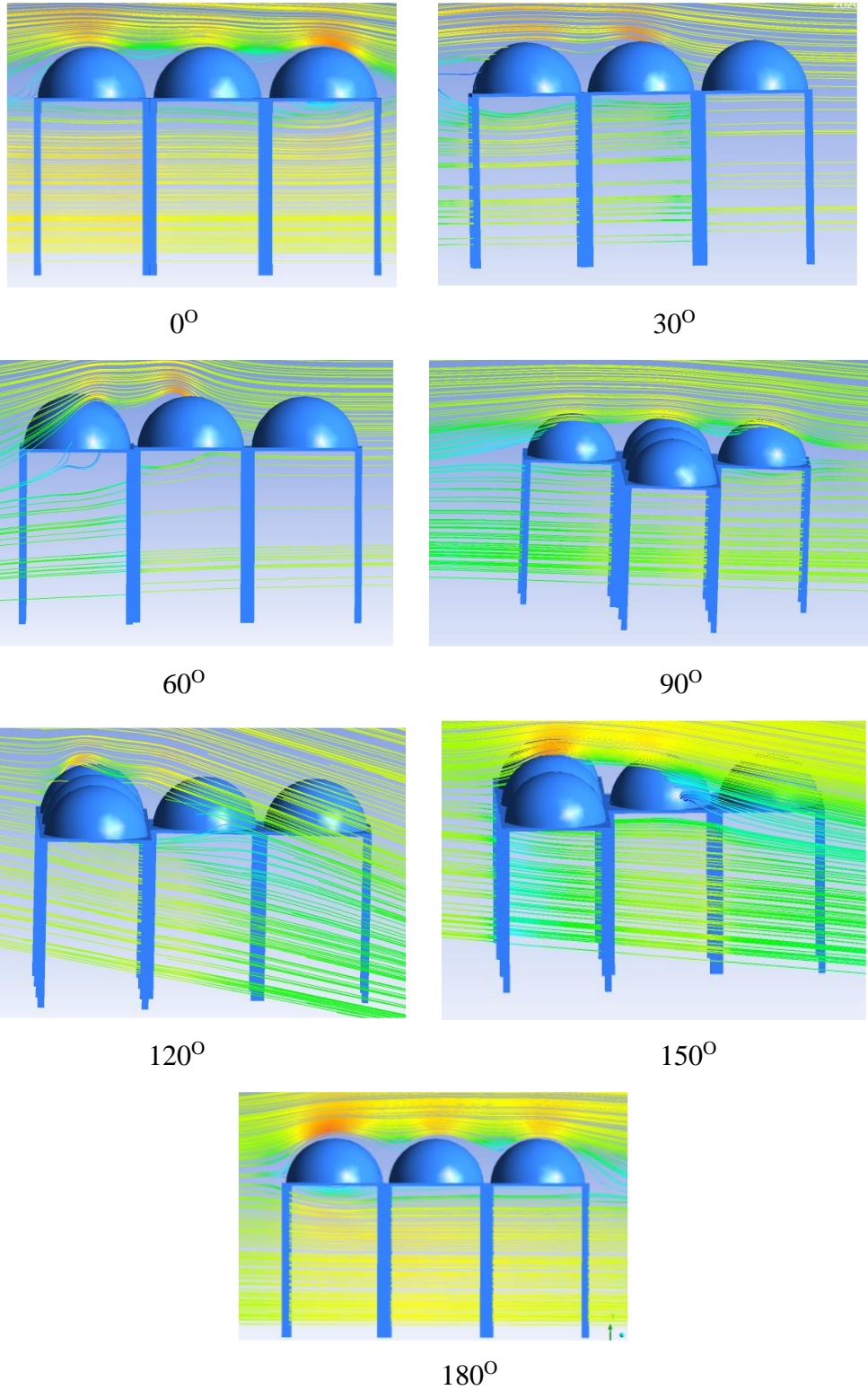


**Fig 5. 4 Streamlines for T shape arrangement at 0 mm spacings**

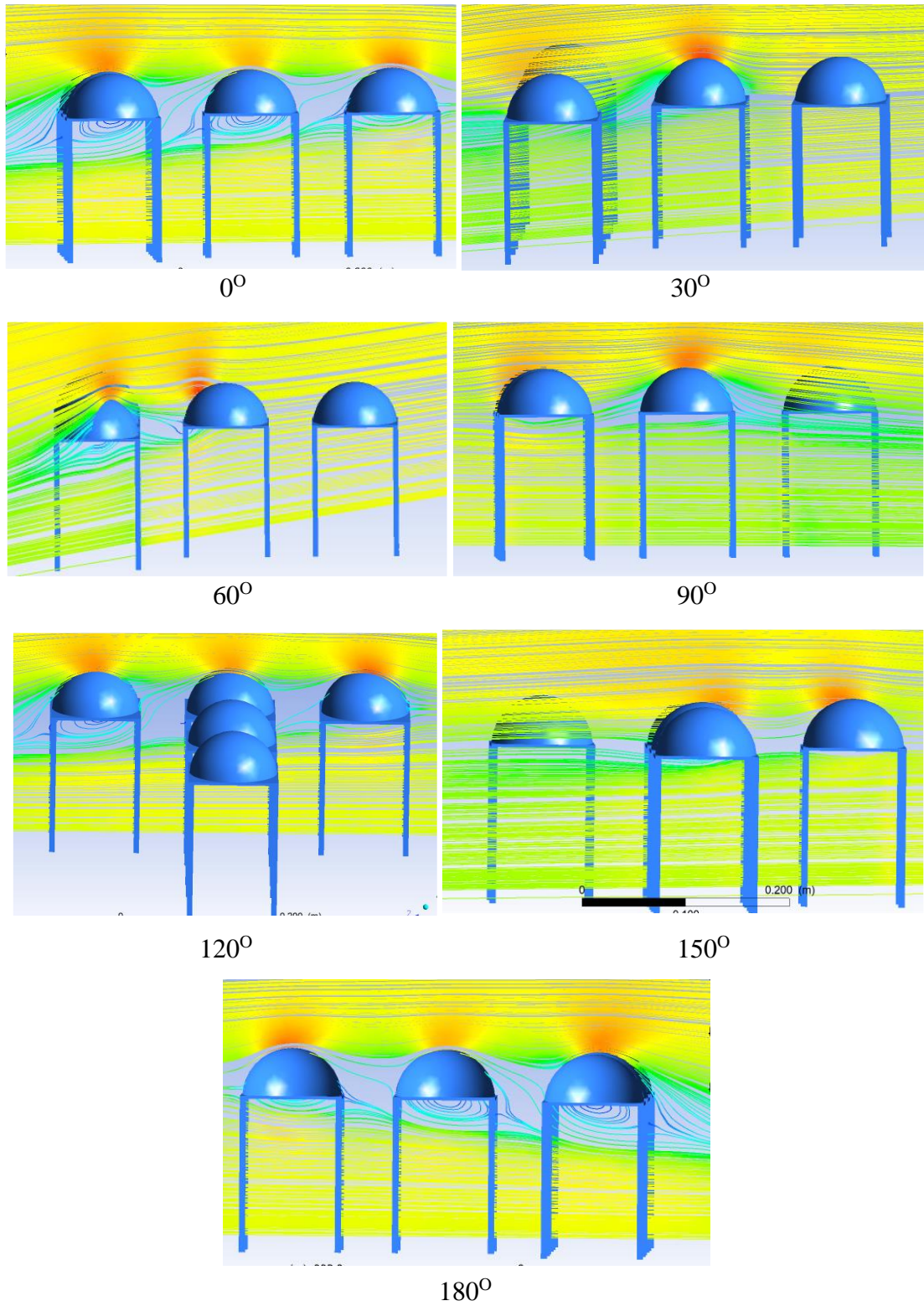


**Fig 5. 5 Streamlines for T shape arrangement at 50 mm spacing**



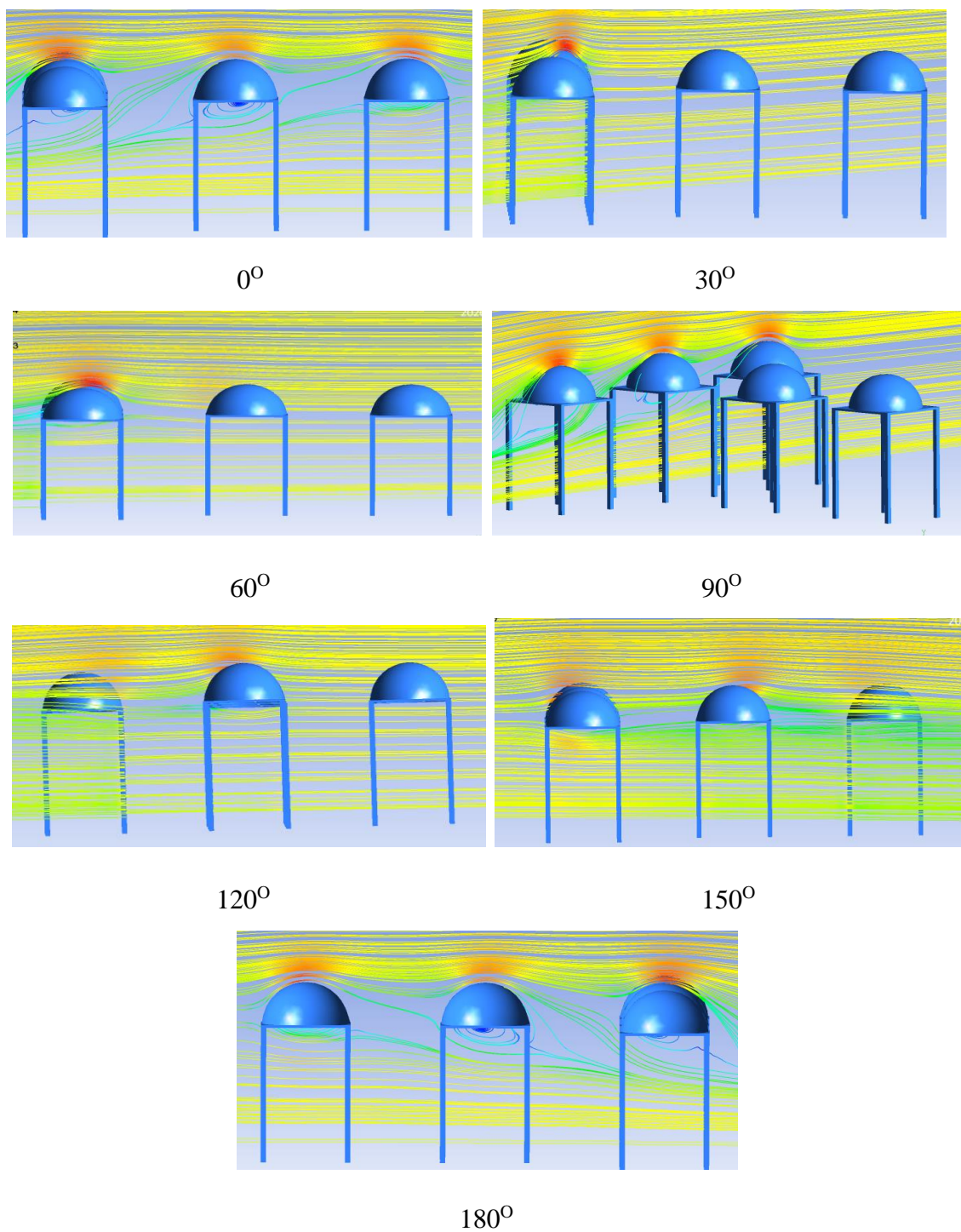


**Fig 5. 6 Streamlines for T shape arrangement at 100 mm spacings**

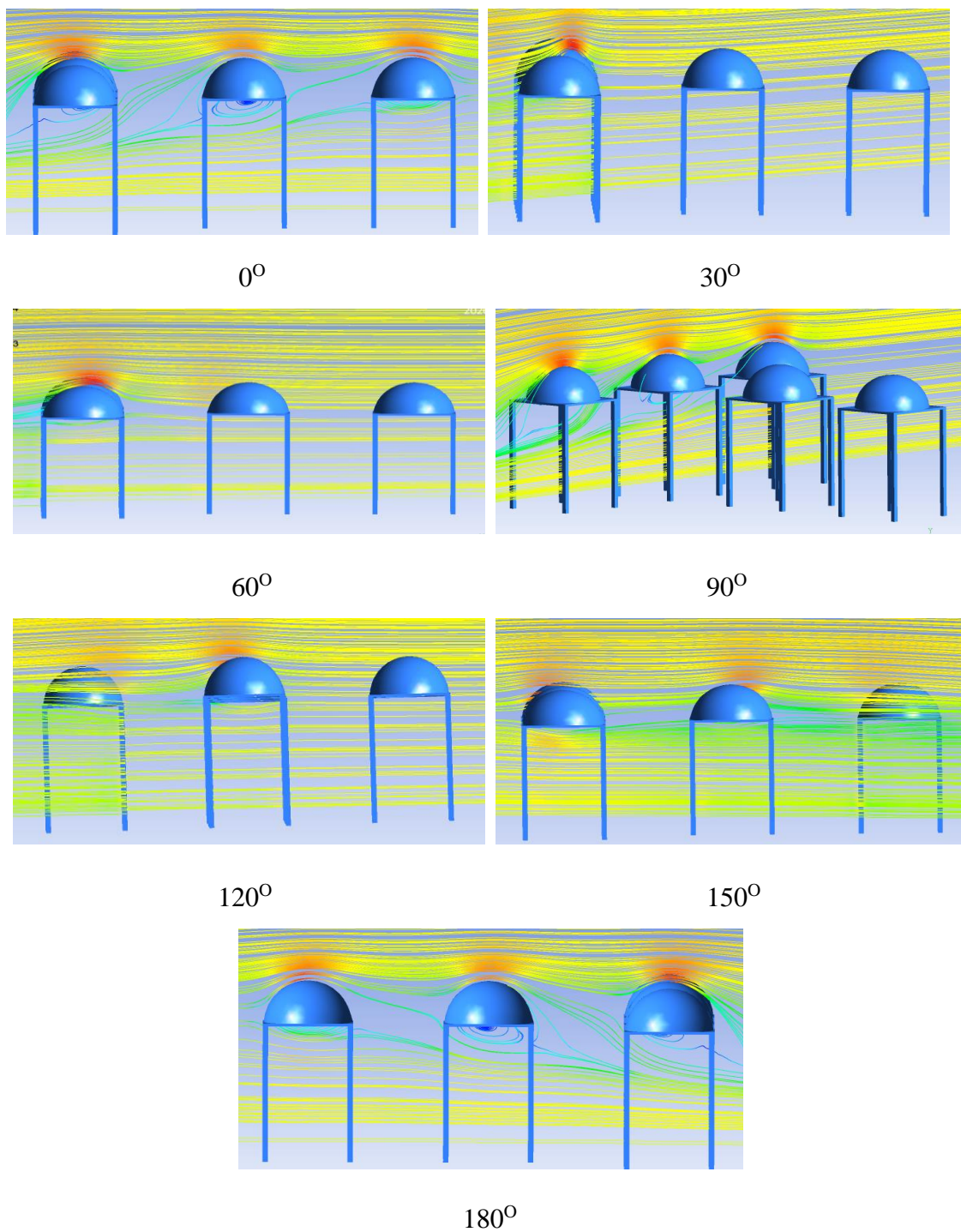


**Fig 5. 7 Streamlines for T shape arrangement at 150 mm spacings**

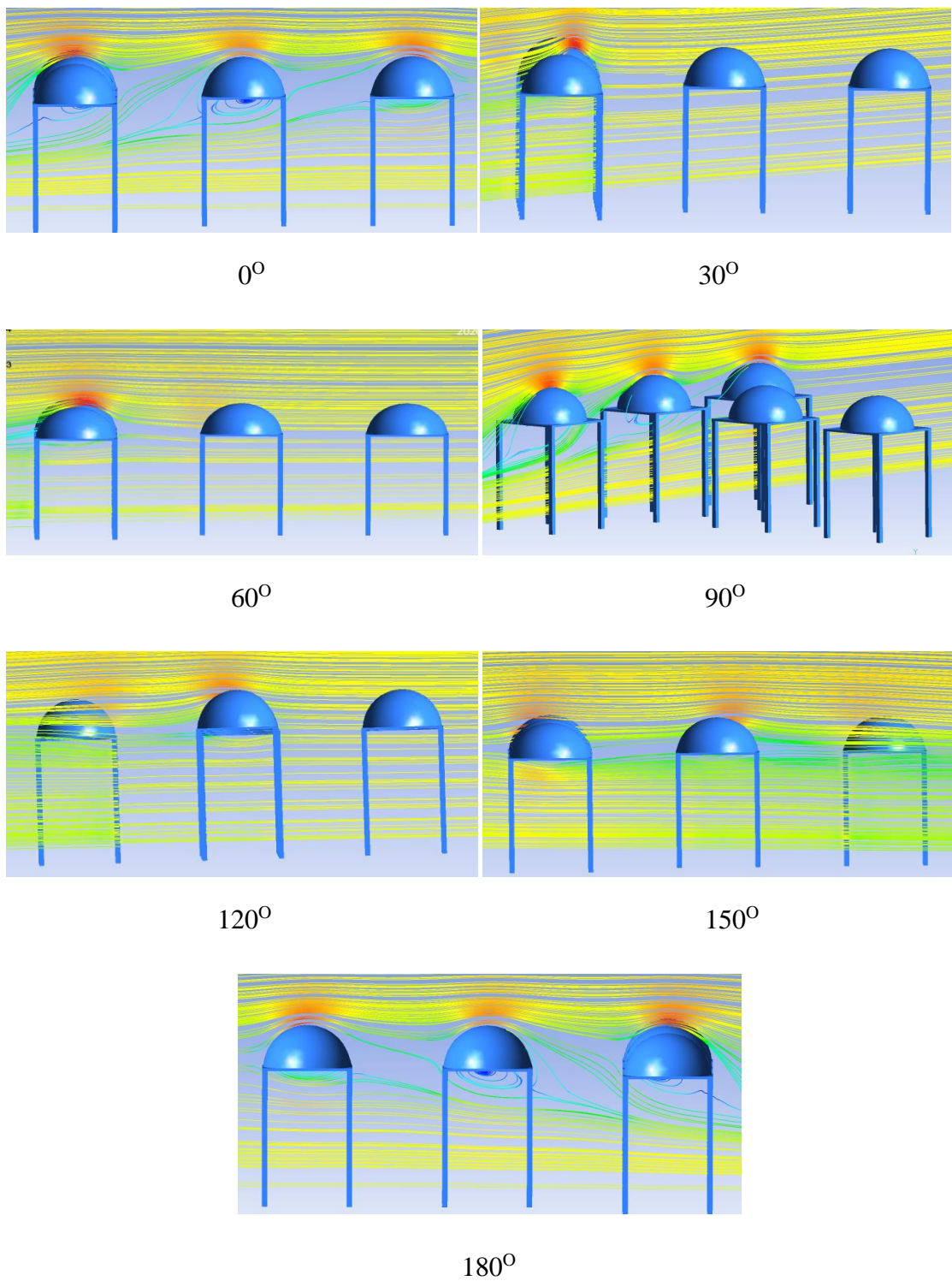


**Fig 5. 8 Streamlines for T shape arrangement at 200 mm spacings**



## 5.4 BUILDING ARRANGED IN L- SHAPE CONFIGURATION

For the arrangement of building arranged in L shape configuration, the wind incidence angle is varied from  $0^\circ$  to  $360^\circ$  at an interval of 30 degree and the spacing between the building is varied at a distance of 0 ,b/2,b,3b/2 and 2 b where b is the width of the isolated building i.e. 0mm,50mm,100mm,150mm and 200mm.

### 5.4.1 COEFFICIENT OF PRESSURE (Cp)

- For 0 mm spacing

**Table 5. 6 Coefficient of pressure (Cp) for L - shape configuration at 0 mm spacing**

Cp				
WIA	DOME 1	DOME 2	DOME 3	DOME 4
$0^\circ$	-0.19092	-0.09095	-0.31918	-0.44551
$30^\circ$	-0.41378	-0.14881	-0.38962	-0.3768
$60^\circ$	-0.50408	-0.41798	-0.43997	-0.183
$90^\circ$	-0.47378	-0.45764	-0.33266	-0.14678
$120^\circ$	-0.53894	-0.53287	-0.44965	-0.38873
$150^\circ$	-0.31633	-0.33351	-0.46684	-0.55959
$180^\circ$	-0.16919	-0.01613	-0.29108	-0.50471
$210^\circ$	-0.28454	-0.15111	-0.41992	-0.31783
$240^\circ$	-0.50324	-0.48276	-0.43705	-0.26342
$270^\circ$	-0.4572	-0.43086	-0.35799	-0.26162
$300^\circ$	-0.58809	-0.64131	-0.37693	-0.49742
$330^\circ$	-0.47758	-0.37305	-0.3366	-0.50392
$360^\circ$	-0.19092	-0.09095	-0.31918	-0.44551

It was observed that for 0 mm spacing between the buildings when arranged in L shape configuration the average coefficient of pressure value is found to be negative i.e. suction is acting on the surface of domes.

When the wind angle is varied from  $0^\circ$  to  $360^\circ$  it is observed that for dome 1 the largest magnitude peak negative of Coefficient of pressure  $C_p$  is -0.58809 for  $300^\circ$  Wind incidence angle, for dome 2 the largest magnitude peak negative of Coefficient of pressure  $C_p$  is -0.64131 for  $300^\circ$  wind incidence angle, for dome 3 the largest magnitude peak negative of Coefficient of pressure  $C_p$  is -0.46684 for  $150^\circ$  wind incidence angle and for dome 4  $C_p$  is found to be -0.55959 for  $150^\circ$  WIA.

- **For 50 mm spacing**

**Table 5. 7 Coefficient of pressure ( $C_p$ ) for L shape configuration at 50 mm spacing**

$C_p$				
WIA	DOMES 1	DOMES 2	DOMES 3	DOMES 4
$0^\circ$	-0.27428	-0.21828	-0.33304	-0.47863
$30^\circ$	-0.38146	-0.31413	-0.42321	-0.38622
$60^\circ$	-0.50061	-0.39936	-0.42564	-0.33446
$90^\circ$	-0.46604	-0.4914	-0.32316	-0.29782
$120^\circ$	-0.45969	-0.50693	-0.50002	-0.39468
$150^\circ$	-0.37795	-0.40252	-0.50072	-0.47826
$180^\circ$	-0.29783	-0.22314	-0.30538	-0.48263
$210^\circ$	-0.3724	-0.3469	-0.4421	-0.36978
$240^\circ$	-0.44827	-0.44888	-0.44325	-0.37036
$270^\circ$	-0.45853	-0.49112	-0.34344	-0.31241
$300^\circ$	-0.54067	-0.4725	-0.38094	-0.46806
$330^\circ$	-0.48799	-0.42391	-0.38621	-0.48829
$360^\circ$	-0.27428	-0.21828	-0.33304	-0.47863

It was observed that for 50 mm spacing between the buildings when arranged in L shape configuration the average coefficient of pressure value is found to be negative i.e.

suction is acting on the surface of domes and the negative  $C_p$  value was found to be reduced by 9.72 % in comparison to values of  $C_p$  for 0 mm spacing.

When the wind angle is varied from  $0^\circ$  to  $360^\circ$  it is observed that for dome 1 the largest magnitude peak negative of Coefficient of pressure  $C_p$  is -0.54067 for  $300^\circ$  Wind incidence angle, for dome 2 the largest magnitude peak negative of Coefficient of pressure  $C_p$  is -0.50693 for  $120^\circ$  wind incidence angle, for dome 3 the largest magnitude peak negative of Coefficient of pressure  $C_p$  is -0.50072 for  $150^\circ$  wind incidence angle and for dome 4  $C_p$  is found to be -0.48829 for  $330^\circ$  WIA.

- **For 100 mm spacing**

**Table 5. 8 Coefficient of pressure ( $C_p$ ) for L shape configuration at 100 mm spacing**

$C_p$				
WIA	DOME 1	DOME 2	DOME 3	DOME 4
$0^\circ$	-0.3432	-0.33462	-0.368	-0.45147
$30^\circ$	-0.39895	-0.3715	-0.4639	-0.454
$60^\circ$	-0.4836	-0.42244	-0.45191	-0.40953
$90^\circ$	-0.44171	-0.47971	-0.37097	-0.37384
$120^\circ$	-0.44997	-0.48085	-0.48957	-0.42077
$150^\circ$	-0.4238	-0.43459	-0.51674	-0.47577
$180^\circ$	-0.36764	-0.28585	-0.3435	-0.49159
$210^\circ$	-0.41886	-0.4147	-0.46685	-0.39558
$240^\circ$	-0.4367	-0.46482	-0.4261	-0.42791
$270^\circ$	-0.42814	-0.46534	-0.37882	-0.36068
$300^\circ$	-0.48667	-0.4715	-0.39688	-0.46207
$330^\circ$	-0.46988	-0.45667	-0.42343	-0.49192
$360^\circ$	-0.3432	-0.33462	-0.368	-0.45147



It was observed that for 100 mm spacing between the buildings when arranged in L shape configuration the average coefficient of pressure value is found to be negative i.e. suction is acting on the surface of domes and the negative Cp value was found to be reduced by 12.40 % in comparison to values of Cp for 0 mm spacing.

When the wind angle is varied from 0° to 360 it is observed that for dome 1 the largest magnitude peak negative of Coefficient of pressure Cp is -0.48667 for 300° Wind incidence angle, for dome 2 the largest magnitude peak negative of Coefficient of pressure Cp is -0.48085 for 120° wind incidence angle, for dome 3 the largest magnitude peak negative of Coefficient of pressure Cp is -0.51674 for 150° wind incidence angle and for dome 4 Cp is found to be -0.49192 for 330° WIA.

- **For 150 mm spacing**

**Table 5. 9 Coefficient of pressure (Cp) for L shape configuration at 150 mm spacing**

Cp				
WIA	DOME 1	DOME 2	DOME 3	DOME 4
0°	-0.35981	-0.35498	-0.41074	-0.45819
30°	-0.40955	-0.43834	-0.4232	-0.4378
60°	-0.47785	-0.45377	-0.45343	-0.40465
90°	-0.44463	-0.45887	-0.37164	-0.38477
120°	-0.45464	-0.46341	-0.47911	-0.42149
150°	-0.42668	-0.45332	-0.49316	-0.459
180°	-0.4023	-0.34766	-0.37333	-0.45887
210°	-0.42587	-0.44961	-0.48146	-0.41881
240°	-0.44034	-0.44307	-0.47283	-0.4356
270°	-0.44803	-0.44642	-0.40786	-0.38379
300°	-0.46206	-0.46848	-0.4282	-0.47385
330°	-0.45809	-0.45594	-0.43359	-0.47057
360°	-0.35981	-0.35498	-0.41074	-0.45819

It was observed that for 150 mm spacing between the buildings when arranged in L shape configuration the average coefficient of pressure value is found to be negative i.e. suction is acting on the surface of domes and the negative Cp value was found to be reduced by 15.18% in comparison to values of Cp for 0 mm spacing.

When the wind angle is varied from  $0^\circ$  to  $360^\circ$  it is observed that for dome 1 the largest magnitude peak negative of Coefficient of pressure Cp is -0.47785 for  $60^\circ$  Wind incidence angle, for dome 2 the largest magnitude peak negative of Coefficient of pressure Cp is -0.46848 for  $300^\circ$  wind incidence angle, for dome 3 the largest magnitude peak negative of Coefficient of pressure Cp is -0.49316 for  $150^\circ$  wind incidence angle and for dome 4 Cp is found to be -0.47385 for  $300^\circ$  WIA.

- **For 200 mm spacing**

**Table 5. 10 Coefficient of pressure (Cp) for L shape configuration at 200 mm spacing**

Cp				
WIA	DOME 1	DOME 2	DOME 3	DOME 4
$0^\circ$	-0.38044	-0.37238	-0.41081	-0.46404
$30^\circ$	-0.42198	-0.46077	-0.46312	-0.44203
$60^\circ$	-0.4639	-0.46966	-0.45362	-0.40236
$90^\circ$	-0.43355	-0.43332	-0.38138	-0.38966
$120^\circ$	-0.44327	-0.45627	-0.47124	-0.42502
$150^\circ$	-0.42382	-0.4481	-0.48196	-0.4645
$180^\circ$	-0.40008	-0.35867	-0.37728	-0.45592
$210^\circ$	-0.42817	-0.43545	-0.48217	-0.43837
$240^\circ$	-0.45563	-0.4522	-0.4522	-0.4531
$270^\circ$	-0.42644	-0.43971	-0.39781	-0.36756
$300^\circ$	-0.46539	-0.47158	-0.41958	-0.47227
$330^\circ$	-0.46928	-0.44761	-0.42479	-0.48124
$360^\circ$	-0.38044	-0.37238	-0.41081	-0.46404

It was observed that for 200 mm spacing between the buildings when arranged in L shape configuration the average coefficient of pressure value is found to be negative i.e. suction is acting on the surface of domes and the negative  $C_p$  value was found to be reduced by 15.58% in comparison to values of  $C_p$  for 0 mm spacing.

When the wind angle is varied from  $0^\circ$  to  $360^\circ$  it is observed that for dome 1 the largest magnitude peak negative of Coefficient of pressure  $C_p$  is -0.46928 for  $330^\circ$  Wind incidence angle, for dome 2 the largest magnitude peak negative of Coefficient of pressure  $C_p$  is -0.47158 for  $300^\circ$  wind incidence angle, for dome 3 the largest magnitude peak negative of Coefficient of pressure  $C_p$  is -0.48217 for  $210^\circ$  wind incidence angle and for dome 4  $C_p$  is found to be -0.48124 for  $330^\circ$  WIA.

#### **5.4.2 VELOCITY STREAMLINES**

As discussed earlier, streamline in a fluid is an imaginary line whose tangent at any point depicts the direction of a fluid particle's velocity at that position. Streamlines are the fluid flow directions, around bodies and in channels. It is a very important parameter that indicates what the flow conditions are, laminar, turbulent or separated. It indicates what is going on and where corrections are needed. Because various flow patterns are observed for buildings, and it is due to the variation in the plan shape of the building, it is necessary to observe for velocity streamlines in order to determine behaviour of wind surrounding the building.

The wind flow streamlines for the arrangement of L shape model for different spacing's from 0 mm to 200 mm model are presented in the Fig 5.4 to Fig 5.8 respectively. We can clearly see from the figures shown below that the streamlines vary with the wind incidence angle which signifies that the pressure distribution due to wind load is highly affected by certain factors on the roof of low-rise building are wind characteristics such as vortex, flow separation, stagnation, flow recirculation and flow reattachment.

It can be observed that the flow separates at the outer edge of the roofs and sides of the buildings, and the split layers of fluid move into the surrounding fluid. When the spacing is increased for the buildings, these layers may be able to rejoin to the surface.

As a result, the separation is repeated at the roof's and sides' downwind borders. These layers are found to eventually converge on the wake axis, resulting in a very imprecisely defined area known as a cavity, regardless of how long or short the building is. The separating streamline emerges from the roof edge on the upwind and above sides. The reattachment streamline runs from the roof edge on the downwind side. Separating streamlines are not the same as reattachment streamlines in two-dimensional flows. The streamlines that emanate from the corners also serve to frame the hollow laterally. It can be seen that the flow inside this roughly ellipsoidal cavity has extremely high turbulence intensity and a low mean velocity, and it regularly reverses direction.

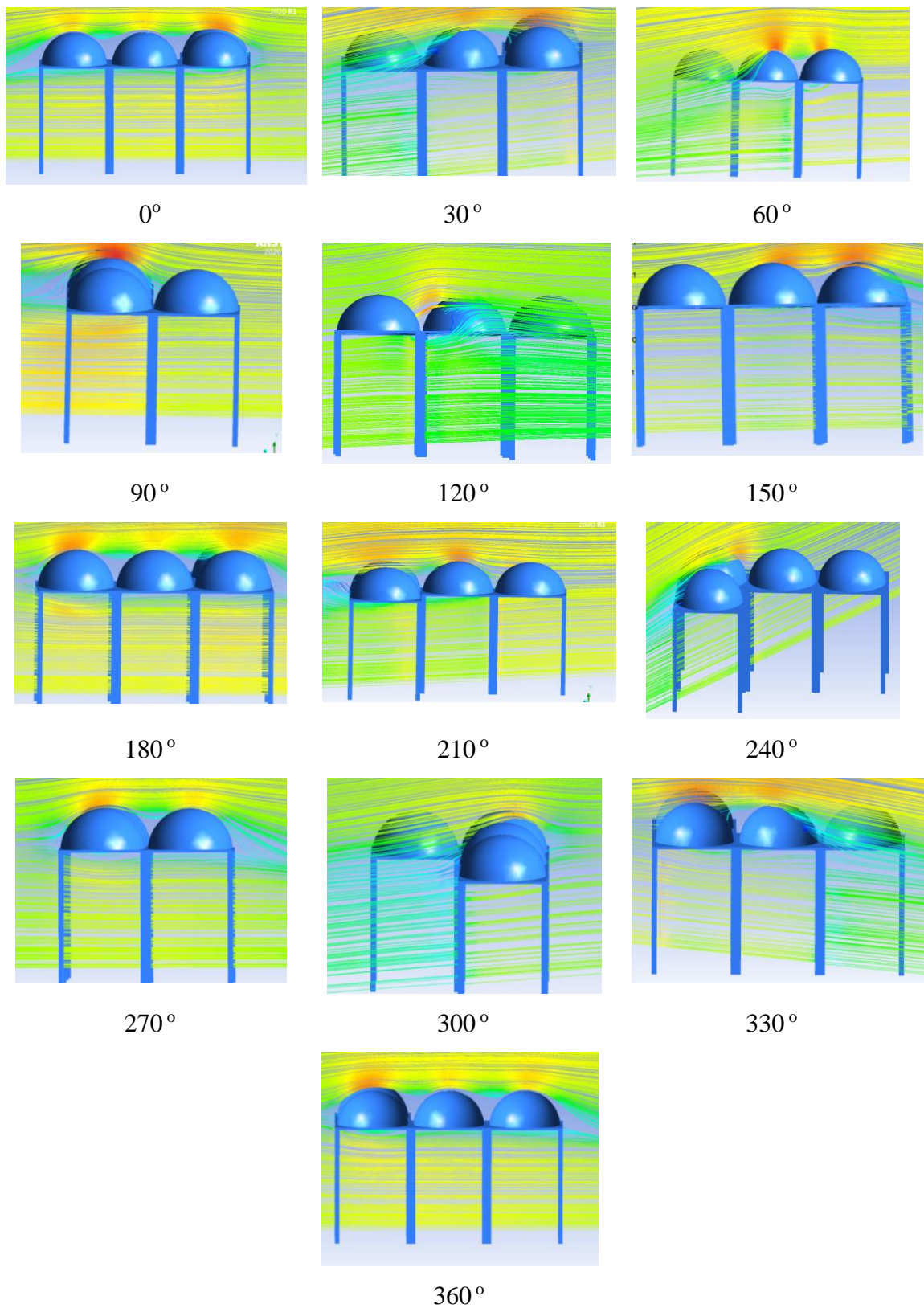


**Fig 5. 9 Streamlines for L shape arrangement at 0mm spacing**

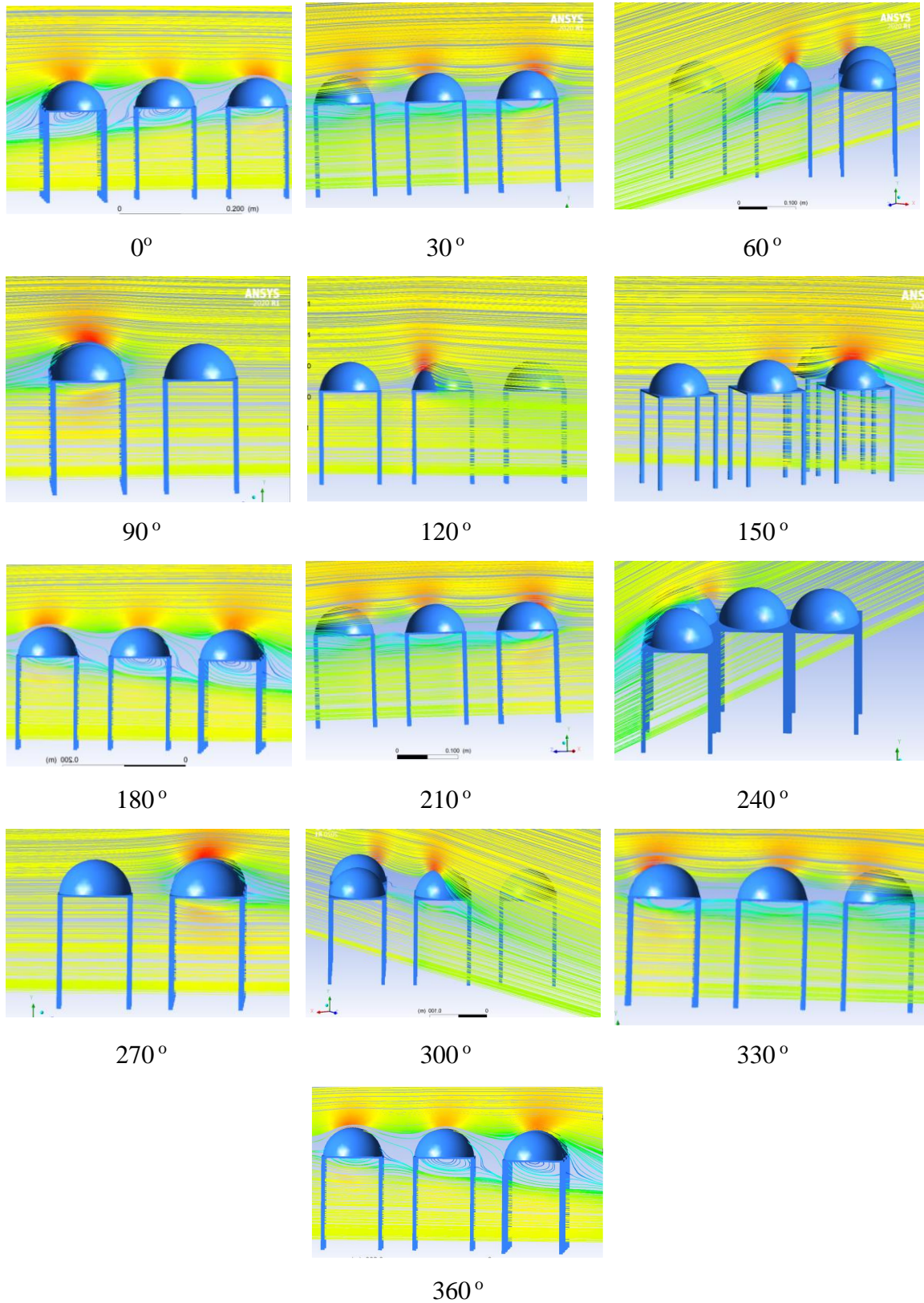


**Fig 5. 10 Streamlines for L shape arrangement at 50mm spacing**



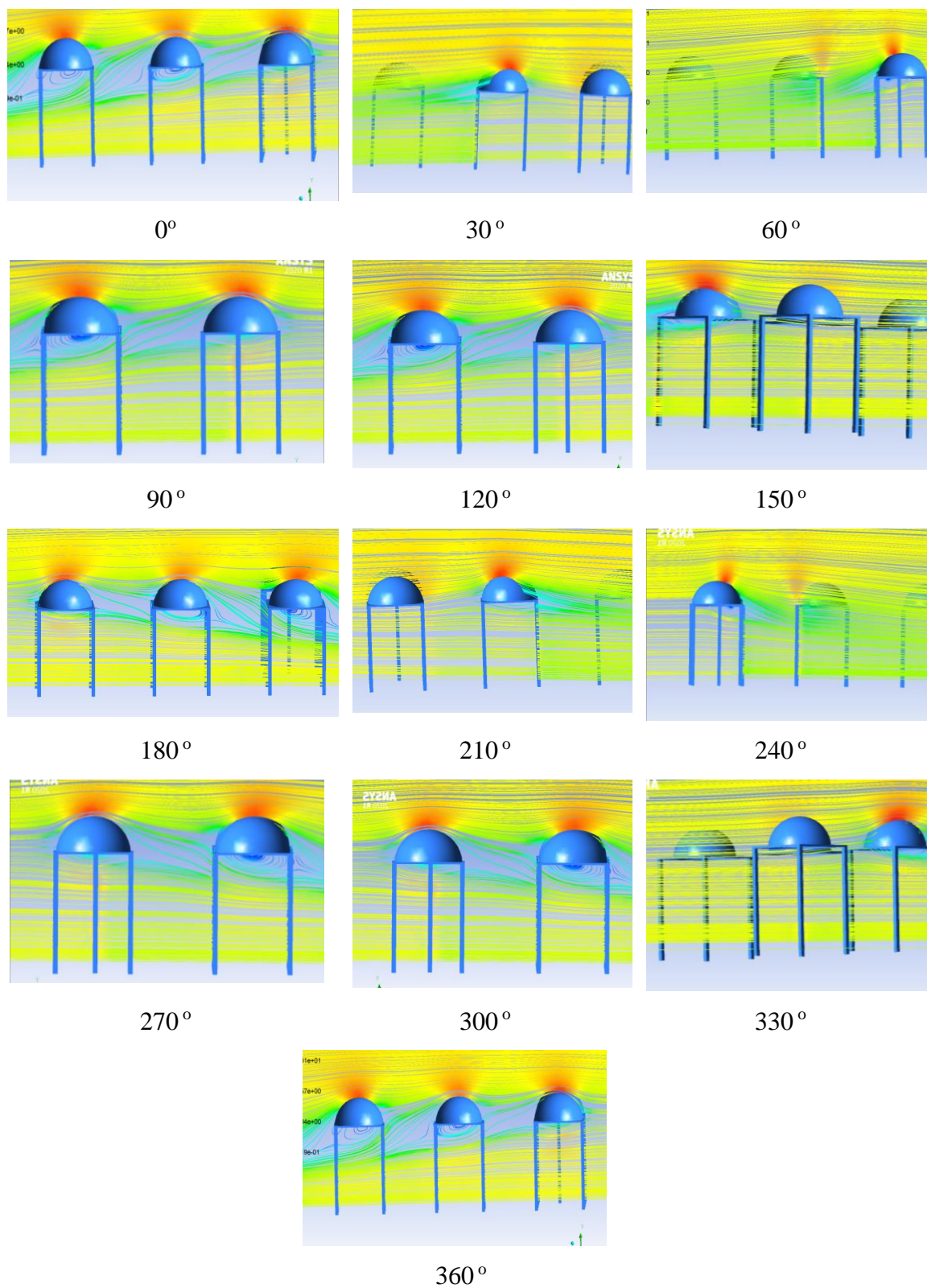


**Fig 5. 11 Streamlines for L shape arrangement at 100mm spacing**

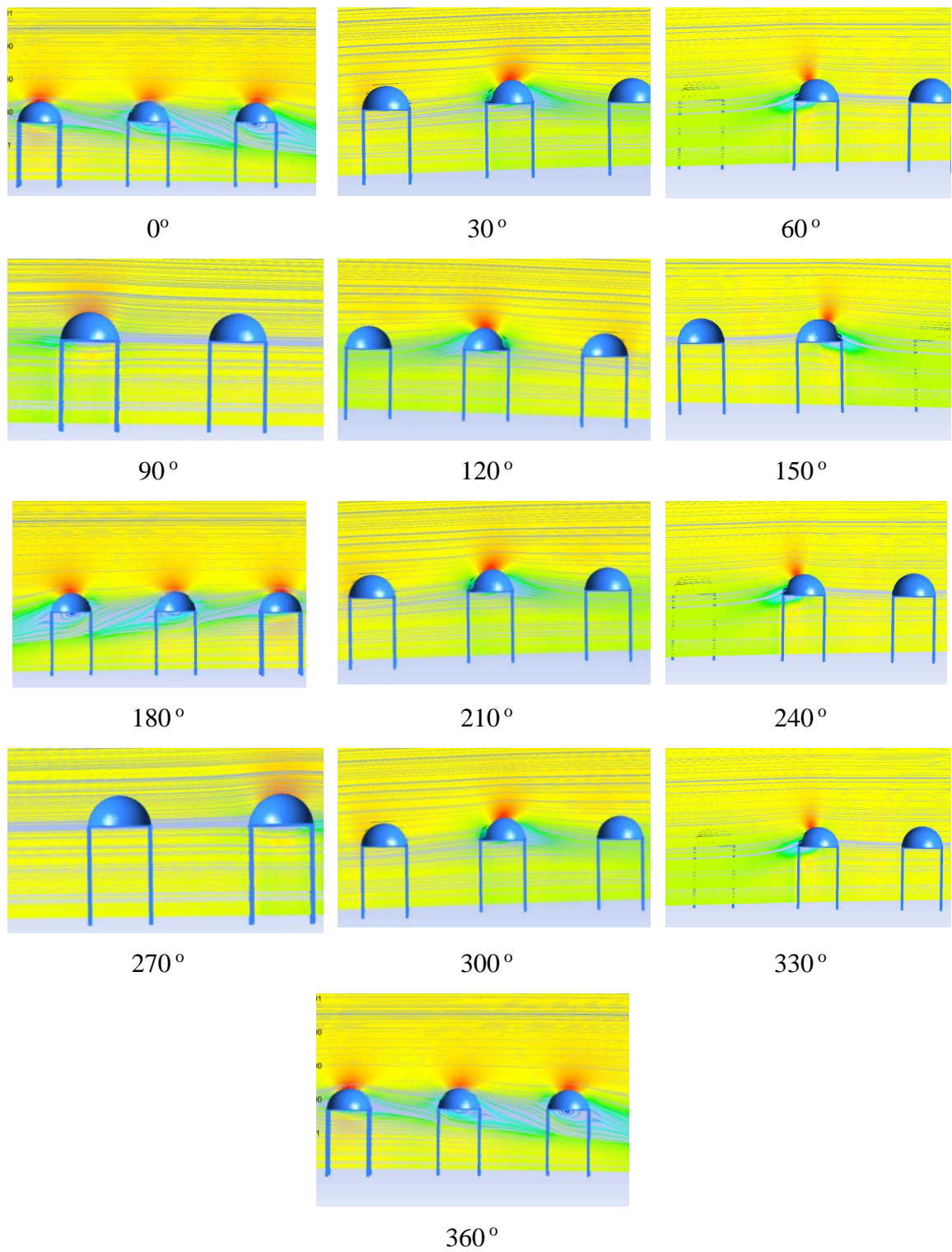


**Fig 5. 12 Streamlines for L shape arrangement at 150 mm spacing**



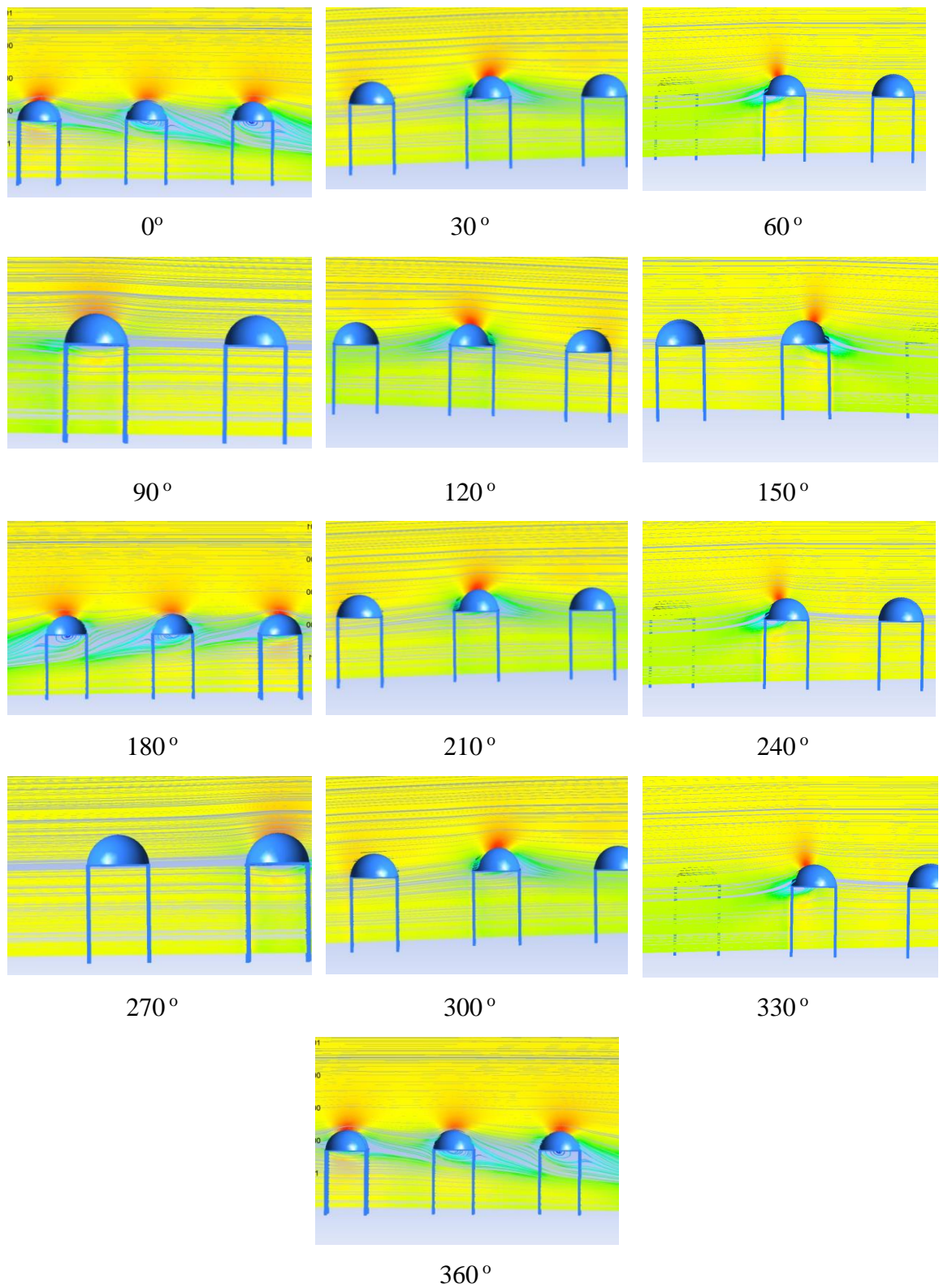


**Fig 5. 13 Streamlines for L shape arrangement at 200 mm spacing**

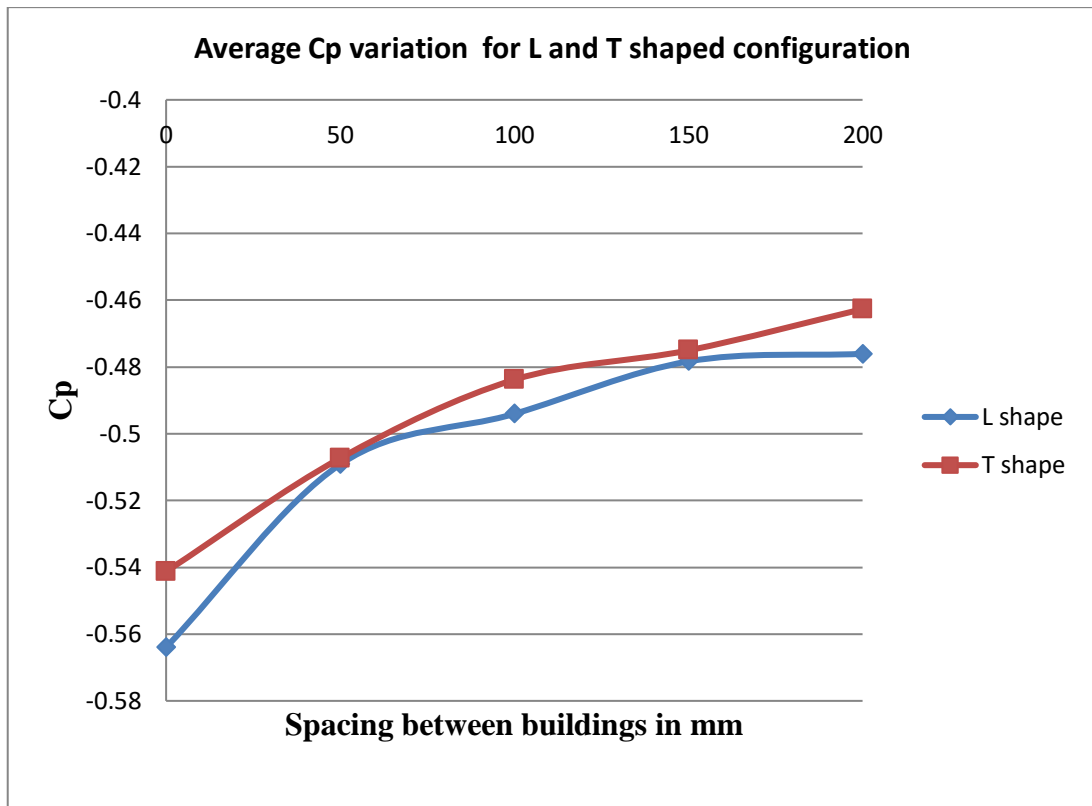


**Fig 5. 14 Average Cp variation for different spacing between the buildings**

The graph above demonstrates how the average coefficient of pressure varies with the distance between buildings. The value of negative Cp was observed to decrease as the spacing between the buildings was increased from 0 mm to 200 mm for each 50 mm increase in the distance, as shown in the graph for both the building models arranged in L and T shape configuration. This shows that the suction value was found to reduce with the influence of surrounding building as the distance between the buildings tends to increase.

## **CHAPTER 6**

### **CONCLUSION**

The effect of wind on the surface of isolated, L shape and T shape domical roofs for the wind incidence angle of  $0^\circ$  to  $360^\circ$  for L shape and  $0^\circ$  to  $180^\circ$  for T shape for the variation of spacing have been investigated in this study to determine the wind pressure coefficient using ANSYS CFX software. The SST modelling technique applied numerical simulation using CFD approach holds in good agreement with the IS code 875 part 3 result and capable of simulating turbulence effect inside wind tunnel. The purpose of the research was to find the pressure distribution on the roof of the building, with the help of coefficient of pressure for the domical roof was analyzed.

A dimensionless quantity known as  $C_p$  represents the relationship between the wind velocity and pressure generated at the building's surface. After considering the geographical location, terrain conditions and shielding effect, the static and design wind pressure are measured at the height of the point considered.

For the variation of spacing, the average coefficient of pressure acting on each dome was found, and it was observed that the average pressure acting on the dome surface is suction for isolated, L shape and T shape domical roofs. The maximum negative value of the pressure is found to be on the centre of the domes which are directly hit by the wind and the value is found to be decrease in the corner region.

The velocity streamlines are depicted in the elevation using the pictorial representation. Because various flow patterns are observed for buildings, and it is due to the variation in the plan shape of the building, it is necessary to observe for velocity streamlines in order to determine behaviour of wind surrounding the building.

The value of negative  $C_p$  was observed to decrease as the spacing between the buildings was increased from 0 mm to 200 mm for each 50 mm increase in the distance for both the building models arranged in L and T shape configuration. It was found that the

suction value was found to reduce with the influence of surrounding building as the distance between the buildings tends to increase.

Buildings located in realistic environments may experience wind loads that differ significantly from buildings situated in isolated environments as studied. In addition to the geometry and arrangement of these structures, their orientation towards the flow direction, and terrain conditions upstream, neighbouring structures may either decrease or increase flow-induced forces on a building. These low-rise structures are exposed to the atmospheric wind speed that is highly prone to uplift pressure. The finding is useful for structural engineers when designing the structure of a low-rise building. As a result, it is important for designers and planners to study the wind induced response of the buildings.

## REFERENCES

- [1] T.J. Taylor, "Wind pressures on a hemispherical dome", *Journal of Wind Engineering and Industrial Aerodynamics*, 40 199-213, 1991.
- [2] R P Hoxey; A P Robertson; B Basara; A Younis, "Geometric parameters that affect wind loads on low-rise buildings: full-scale and CFD experiments ", *Journal of Wind Engineering and Industrial Aerodynamics*, 50 243-252, 1993.
- [3] P.J. Richards, R.P Hoxey, B.D. Connella, D.P. Lande, " Wind-tunnel modelling of the Silsoe Cube", *Journal of Wind Engineering and Industrial Aerodynamics* , 95 1384–1399, 2007.
- [4] M.M. Tavakol , M. Yaghoubi , M. Masoudi Motlagh, "Air flow aerodynamic on a wall-mounted hemisphere for various turbulent boundary layers", *Experimental Thermal and Fluid Science*, 34 ,538–553 ,2010.
- [5] Alireza Fiouz and Mohammad Ebrahim Karbaschi, "Effect of wind loading on spherical single layer space truss steel domes ", *International Journal of Physical Sciences* Vol. 7(16), pp. 2493 - 2505, 16 April, 2012.
- [6] Yong Chul Kim; Akihito Yoshida; Yukio Tamura, "Influence of Surrounding Buildings on Wind Loads Acting on Low-Rise Building", *J. Struct. Eng.*, 139:275-283, 2013.
- [7] Peng Zhou, Baijian Tang, Ping Liu, Gaoming Zheng, "Study on Wind Load Distribution on the Surface of Dome Structure", *Journal of Physics: Conf. Series* 1176 ,052056, 2019.
- [8] Astha Verma, Ashok K. Ahuja, "Wind Pressure Distribution on Domical Roofs", *International Journal of Engineering and Applied Sciences (IJEAS)* ISSN: 2394-3661, Volume-2, Issue-5, May 2015.
- [9] Astha Verma, Ashok K. Ahuja, "Wind Pressure Distribution on Rectangular Plan Buildings with Multiple Domes", *International Journal of Engineering and Technical Research (IJETR)* ISSN: 2321-0869 (O) 2454-4698 (P), Volume-3, Issue-7, July 2015.

- [10] Astha Verma and Ashok Kumar Ahuja, "Wind pressure distribution on low-rise buildings with cylindrical roofs", *Proceedings of International Structural Engineering and Construction*, 2015 .
- [11] Hossein Sadeghi, Mahmoud Heristchian, Armin Aziminejad, Hoshyar Nooshin, "Wind effect on grooved and scallop domes", *Engineering Structures* ,148 ,436–450, 2017.
- [12] Jagbir Singh and Roy Amrit Kumar , "Wind loads on roof of low-rise buildings", *Computational Engineering and Physical Modelling* ,1-1 , 01-16, 2018.
- [13] Nourhan Sayed Fouad, Gamal Hussien Mahmoud, Nasr Eid , "Comparative study of international codes wind loads and CFD results for low rise buildings ", *Alexandria Engineering Journal* , 2018.
- [14] R.H. Ong, L. Patruno, D .Yeo, Y.Hee, K.C.S. Kwok, "Numerical simulation of wind-induced mean and peak pressures around a low-rise structure ", *Engineering Structures*, 214 ,110583, 2020.
- [15] Stathopoulos T, "Numerical Simulation of Wind-induced Pressure on Buildings of Various Geometries", *J. WindEngg. Indus. Aerodynam*, vol. 46 & 47, pp. 419–430, 1993.
- [16] Kushal T, " Effect of plan shapes on Response of Tall buildings", *IIT Roorkee, India*.
- [17] Gregory A. Kopp; Jon K. Galsworthy; Jeong Hee Oh, " Horizontal Wind Loads on Open-Frame, Low-Rise Buildings ", *J. Struct. Eng*, 136:98-105, 2010.
- [18] Jagbir Singh and Roy Amrit Kumar , "Wind loads on roof of low-rise buildings ", *Computational Engineering and Physical Modelling* ,1-1 ,01-16, 2018.
- [19] R. Ahlawat and A. Ahuja, "Wind Loads on T Shape Tall Buildings", *Journal of Academia and Industrial Research*, vol. 24, no. 1, p. 257922, 2015.
- [20] R. Ahlawat and A. K. Ahuja, "Wind loads on Y plan shape tall building", *International Journal of Engineering and Applied Sciences*, vol. 2, no. 4, p. 257946, 2015.

- [21] R. Raj and A. K. Ahuja, "Wind Loads on Cross Shape Tall Buildings", *Journal of Academia and Industrial Research (JAIR)*, vol. 2, no. 2, pp. 111–113, 2013.
- [22] P. K. R. in Ehsan Vafaeihosseini, Azadeh Sagheb, "Computational Fluid Dynamics Approach for Wind Analysis of Highrise Buildings", no. January, 2013.
- [23] R. K. Meena, G. P. Awadhiya, A. P. Paswan, and H. K. Jayant, "Effects of Bracing System on Multistoreyed Steel Building ", *IOP Conference Series: Materials Science and Engineering*, vol. 1128, no. 1, p. 012017, doi: 10.1088/1757-899X/1128/1/012017, Apr. 2021.
- [24] S. Pal, R. Raj, and S. Anbukumar, "Comparative study of wind induced mutual interference effects on square and fish-plan shape tall buildings", *Sadhana*, vol. 0123456789, doi: 10.1007/s12046-021-01592-6, 2021.
- [25] D. S. K. Verma, A. Roy, S. Lather, and M. Sood, "CFD Simulation for Wind Load on Octagonal Tall Buildings", *International Journal of Engineering Trends and Technology*, vol. 24, no. 4, pp. 211–216, doi: 10.14445/22315381/ijett-v24p239, 2015.
- [26] B.E. Launder, D.B. Spalding, "Lectures in mathematical models of turbulence", *Academic Press*, London, England ,1972.
- [27] Nichols R.H. , " Turbulence Models and Their Application to Complex Flows", *University of Alabama, Birmingham, University of Alabama* ,2010.
- [28] Franke, J., Hirsch, C., Jensen, A. G., Krus, H.W., Schatzmann, M., Westbury P.S., Miles S. D., Wisse, J.A. and Wright, N. G., "Recommendations on the Use of CFD in Wind Engineering. Cost Action C, (January), pp.1–11, 2004.
- [29] Lo, Y.L., Kim, Y.C. and Li, Y.C. , "Downstream interference effect of high-rise buildings under turbulent boundary layerflow", *J. Wind Eng. Ind. Aerod.*, 159, 19-35,2016.
- [30] Kar, R., Dalui, S.K. and Bhattacharya, S., " An efficient optimization approach for wind interference effect on octagonal tall building", *Wind and Structures*, Vol. 28, No. 2 ,111-128,2019.

- [31] Menter FR, "Two-equation eddy viscosity turbulence models for engineering applications", AIAA Journal 32(8):269–89.
- [32] AS/NZS: 1170.2, "Structural design actions, part 2: wind actions", Standards Australia/Standards New Zealand, Sydney, Wellington, 2011.
- [33] ASCE: 7-16, "Minimum design loads for buildings and other structures", Structural Engineering Institute of the American Society of Civil Engineering, Reston, 2016.
- [34] IS: 875(Part-3), "Indian standard code of practice for design loads (other than earthquake) for buildings and structures, part 3 (wind loads)", Bureau of Indian Standards, New Delhi, 2015.



## **PUBLICATIONS**

- [1].Jyoti Singh, Ritu Raj,“ Estimation of aerodynamic effects on domical roof structure”,4th International Conference on Recent Scientific and Technological Trends ,May 2022 .
- [2].Jyoti Singh, Ritu Raj ,“ Wind Induced Response on Domical Roof Structures”,  
2nd International Conference on Sustainable Materials and Computational Techniques – 2022, May 2022.

PAPER NAME

**2k20ste10 thesis report.pdf**

AUTHOR

**Jyoti Singh**

WORD COUNT

**12793 Words**

CHARACTER COUNT

**63585 Characters**

PAGE COUNT

**73 Pages**

FILE SIZE

**4.2MB**

SUBMISSION DATE

**May 30, 2022 1:26 PM GMT+5:30**

REPORT DATE

**May 30, 2022 1:28 PM GMT+5:30**

### ● 12% Overall Similarity

The combined total of all matches, including overlapping sources, for each database.

- 10% Internet database
- 6% Publications database
- Crossref database
- Crossref Posted Content database
- 7% Submitted Works database

### ● Excluded from Similarity Report

- Small Matches (Less than 14 words)